Title
Signaling and Morphogenesis of the Ascidian Neural Tube

Author
Navarrete, Ignacio Andres

Publication Date
2016

Peer reviewed|Thesis/dissertation

Signaling and Morphogenesis of the Ascidian Neural Tube

By

Ignacio Andres Navarrete

A thesis submitted in partial satisfaction of the

requirements for the degree of

Doctor of Philosophy

in

Molecular and Cell Biology

in the

Graduate Division

of the

University of California, Berkeley

Committee in charge:

Professor Michael S. Levine, Chair

Professor Richard M. Harland

Professor John C. Gerhart

Professor David R. Lindberg

Fall 2016

Abstract

Signaling and Morphogenesis of the Ascidian Neural Tube

by

Ignacio Andres Navarrete

Doctor of Philosophy in Molecular and Cell Biology

University of California, Berkeley

Professor Michael Levine, Chair

Formation of the vertebrate neural tube represents one of the premier examples of morphogenesis in animal development. Here, we investigate this process in the simple chordate, *Ciona intestinalis*. Previous studies have implicated Nodal and FGF signals in the specification of lateral and ventral neural progenitors. We show that these signals also control the detailed cellular behaviors underlying morphogenesis of the neural tube. Live imaging experiments show that FGF controls the intercalary movements of ventral neural progenitors, while Nodal is essential for the characteristic stacking behavior of lateral cells. Ectopic activation of FGF signaling is sufficient to induce intercalary behaviors in cells that have not received Nodal. In the absence of FGF and Nodal, neural progenitors exhibit a default behavior of sequential cell divisions, and fail to undergo the intercalary and stacking behaviors essential for normal morphogenesis. Thus, cell specification events occurring prior to completion of gastrulation coordinate morphogenetic movements underlying the organization of the neural tube.

Acknowledgments:

I would like to thank the many people who have made this dissertation possible.

First and foremost is Mike Levine, who supported me till the very end and provided an unparalleled environment for conducting great science. I have also relied on the enduring generosity and kindness of Richard Harland and the Harland Lab, who graciously hosted me for my final year at Berkeley. I would also like to thank the following members of the scientific community who have each assisted me in one way or another: David Jacobs, Ryan Ellingson, David Gold, Peggy Fong, the Levine Lab, John Gerhart, David Lindberg, Craig Miller, Nipam Patel and Matthew Welch. A special thanks goes out to team *Ciona*: Blair Gainous, Phil Abitua, Eileen Wagner, Emma Farley, and Katrina Olson as well as my best friends in the department, Ignacio Gutierrez, Ryan Null, Kevin Tsui, and Emilia Esposito. Additional thanks to Shigeki Fujiwara for generously providing the Nodal perturbation plasmids and Alberto Stolfi for advancing the molecular biology capabilities of the Levine Lab.

I would also like to thank my many wonderful friends who made life worth living during this often difficult process, I love you all. In particular, thank you Anna, you have seen the best and the worst of me.

Finally thank you to my family, Ignacio, Hester, Paul and Apusa, who have always been there for me and are the best family one could ever have.

TABLE OF CONTENTS

Chapter 1: Introduction

Embryonic development is a fascinating aspect of the natural world. During this process, a single cell is transformed into an animal. Moreover, this happens autonomously; both the instructions and machinery to make an animal are already contained within the fertilized egg, and so formation of the animal is merely a matter of activating the developmental program and allowing it to unfold. As if this weren't enough, this process was not designed but refined over millions of years of evolution, diverging again and again to create the diversity of animal life we presently enjoy on earth. Thus, an understanding of development seems one of the keys to understanding our own existence and the life that surrounds us.

Fundamentally, animal development consists of two aspects inseparably linked over the course of the developmental program. One is the behavior of cells including their divisions, changes in size and shape, movements, secretion of molecules, and even death. The other is the achievement of unique identities, some temporary, which allow for the diversity of cell behaviors taking place both during development and in the fully formed animal. One cannot take place without the other. At a minimum a single cell division is required before two identities can coexist from a given lineage. At the same time the very fact that a cell divides is part of its identity. Consequently, the study of development comes down to attempting to understand how these two facets, cell behavior and identity, guided by an organism's genetic heritage, interact through time.

As scientists and humans we are limited, and therefore must uncover this understanding piece by tiny piece. In this dissertation I will present my work on one such piece, the links between cell specification and morphogenesis of the ascidian posterior central nervous system. To place this work in its proper context, the introduction is divided into the following sections. I will begin by introducing the ascidian embryo as a model system for understanding embryonic development. I will then review past work describing how cells of the posterior nervous system come to achieve their unique identities by the onset of neurulation. Finally, I will briefly describe the conceptual links between specification and morphogenesis, including my motivations for the present study.

Ascidian Developmental Biology Research

Ascidians are sessile filter feeders found in marine environments around the world. Adults are characterized by an oral siphon, connected to the pharyngeal basket where food is captured, and an atrial siphon through which filtered water is jettisoned. Fossil evidence suggests that this body plan dates back at least to the Lower Cambrian (Swalla and Smith, 2008). Ascidians are tunicates, or urochordates, which despite wildly divergent adult forms make up the invertebrate phylum closest our own, the vertebrates (Delsuc et al., 2006). This is most evident in the ascidian larva, which, like vertebrates, has a notochord flanked by lateral muscles, a hollow dorsal nerve cord, and ventral endoderm. These similarities were first recognized by Kovalevsky (1866), giving rise to the idea (later championed by Charles Darwin) that the common ancestor of all vertebrates might in fact have looked much like a larval ascidian. While it now seems just

as likely that the ascidian tadpole is the result of an evolutionary simplification rather than a static fossil representing our origins, these distant and highly simplified cousins may still hold some of the answers to the mysteries of our own development and evolution.

Development of the ascidian larvae, from egg to hatching, takes place over an approximately 24 hour period in species such as *Ciona intestinalis.* The majority of cell lineages are invariant, and there are approximately 2,600 cells in the mature tadpole larvae. Development begins when the egg cleaves into left and right halves, with continuous cleavages taking place until the 110-cell stage. At this point gastrulation begins, with vegetal endoderm precursors entering the embryo first, followed by mesodermal muscle and notochord precursor cells. Neurulation immediately follows gastrulation, resulting in a dorsal nerve cord posteriorly and an anterior sensory vesicle homologous to the vertebrate brain. Towards the end of neurulation the tail begins to elongate eventually making up ~4/5 of the total length of the larvae. The larva then hatches, swimming for up to a few days before settling and metamorphosing into the adult form.

Study of ascidian cell lineages was pioneered by Edwin Conklin, who traced cells via direct observation of divisions and devised a system of nomenclature used to this day. His system divides the bi-lateral 8-cell embryo into 4 founder lineages (a-anterior animal, b-posterior animal, A-anterior vegetal and B-posterior vegetal). His 1902 study "organization and cell lineages of the ascidian egg" demonstrated that cells in the early embryo invariably contributed to a particular tissue in the larvae. This led him to the hypothesis that ascidian embryos exhibit "mosaic development" whereby embryonic determinants are gradually segregated at every cell division, eventually causing each blastomere to adopt its ultimate fate. While the idea of strictly mosaic embryonic development has been disproven, the desire to characterize and isolate the ascidian embryonic determinants motivated much of the work that brought ascidian embryology into the molecular era. This can be best appreciated by considering two of the best-studied instances of fate determination in ascidians; primary muscle specification and induction of anterior neural fates.

The search for inherited determinants of a particular fate has been most fruitful in the case of the B-lineage, which gives rise to the majority of larval muscle cells (Nishida, 1986). In addition to his observation that a subset of cells in this lineage gives rise exclusively to muscle, Conklin also observed that these cells preferentially inherit a unique yellow portion of the ooplasm. Later studies confirmed that cells of this lineage eventually differentiate into muscle even when continuously isolated after each round of division, suggesting that these cells do in fact contain determinants sufficient to generate muscle (Nishida, 1992). Furthermore, transplantation of cytoplasmic material from these cells to other blastomeres causes them to express muscle markers at low frequency (Satoh, 1984; Whittaker, 1982). Even with this knowledge, it took until 2001 for the muscle determinants to be isolated and characterized. Relying on earlier clues that the determinant likely consisted of maternally deposited mRNA, Nishida and Sawada (2001) performed a subtractive screen, eventually isolating mRNAs for the Zic finger

transcription factor *Macho-1*. *Macho-1* mRNA proved to be necessary for muscle development in the B-lineage and sufficient to induce muscle development in other lineages, thus ending the search for a muscle determinant nearly 100 years after its existence was proposed.

The first proof that ascidian development does not follow a strictly mosaic developmental plan came with the observation that development of the a4.2 blastomeres into the brain, palps and pigmented sensory organs requires contact with vegetal A4.1 cells (Okado and Takahashi, 1988). Indeed, it had already been observed by Chabry (1887) as well as Rose (1939) that animal blastomeres isolated at the 8-cell stage failed to generate either neurons or the pigmented cells of the sensory vesicle. Subsequent experiments investigating the nature of this induction showed that expression of the early neural marker *Otx* in the a4.2 lineage depends on contact with vegetal blastomeres, demonstrating that the this contact is required for the earliest stages of anterior neural induction (Hudson and Lemaire, 2001).

The search for the molecular nature of the neural inducer also highlights the steady progress of our understanding of embryonic induction. Initial work focused on secreted proteases which were found to induce both pigment cell formation and neural differentiation in isolated animal cells (Okado and Takahashi, 1988; Ortolani et al., 1979). Following this, researchers sought to relate ascidian neural induction to that of vertebrates, where FGF had been interpreted to act as a neural inducer in cultured Xenopus ectodermal cells (Kengaku and Okamoto, 1993; Kengaku and Okamoto, 1995). Indeed, low doses of exogenous FGF were sufficient to induce neuronal ion channels in cleavage arrested a4.2 blastomeres (Inazawa et al., 1998). Further evidence for the importance of FGF came from the loss of neural markers upon FGF inhibition (Kim and Nishida, 2001) and the very rapid activation of *Otx* by FGF in cleavage stage animal explants (Hudson and Lemaire 2001). Work in this area culminated in the discovery that FGF directly regulates enhancers of target genes such as *Otx* via the map kinase (MAPK) pathway and Ets family transcription factors (Bertrand et al., 2003).

Similar progress has been achieved in understanding how other cell identities are achieved. A provisional gene regulatory network has been constructed for the early embryo (Imai et al., 2006), and a combination of continuous refinements (e.g. Hudson et al., 2016; Kodama et al., 2016; Wagner and Levine, 2012) and extension to later developmental stages (e.g. Christiaen et al., 2009; Stolfi and Levine, 2011; Wagner et al., 2014) suggests that we may eventually come to know the molecular basis for specification of each cell at each stage of embryonic development. Meanwhile we are just beginning to investigate how the behaviors of cells are determined by their identities and embryonic context. So far, the intercalation and elongation of the notochord has received the greatest attention (Denker et al., 2015; Kourakis et al., 2014; Veeman et al., 2008), though studies on gastrulation (Sherrard et al., 2010), heart cell migration (Christiaen et al., 2008) and neural tube zippering (Hashimoto et al., 2015) have begun to shed light on these processes as well.

The aim of my dissertation is to begin dissecting the links between cell specification and

morphogenesis of the ascidian tail nerve cord. Unlike the other morphogenetic processes studied so far, nerve cord morphogenesis involves multiple cell types and behaviors. Yet in spite of this apparent complexity, it has a cross section of just four cells, making it perhaps the simplest possible structure of this kind. My work has focused on the lateral and ventral cells of the nerve cord which are both derived from the A-lineage. The sequence of events leading these cells to adopt unique neural identities has been thoroughly dissected and is described below. My work, presented in subsequent chapters, extends this analysis by probing how perturbation of cell specification affects the morphogenetic movements of these cells during neurulation.

The A-line neural lineage

The ascidian central nervous system is derived from three of the four 8-cell stage lineages. Among these, the anterior-vegetal or A-line lineage gives rise to the ventral and lateral portions of the tail nerve cord, trunk ganglion and parts of the sensory vesicle (Figure 1B). This lineage also contributes endoderm, notochord and muscle cells to the larva.

The A-lineage emerges at the 8-cell stage after the animal-vegetal oriented division of the 4-cell embryo. A subsequent round of medial-lateral oriented divisions creates the 16-cell stage at which point zygotic gene expression begins (Figure 1A). At this stage all vegetal blastomeres have accumulated active β-catenin/TCF, which is responsible for the activation of the earliest vegetal domain genes and repression of animal genes. A-line cells are distinguished from the posterior vegetal B-lineage by the absence of maternal Macho-1 (Oda-Ishii et al., 2016). As a result of β-catenin /TCF activity, 3 critical genes are activated in the A-lineage, *FoxD*, *Fgf9/16/20*, and *FoxA* (Hudson et al., 2016).

The next division into the 32-cell stage segregates A-line cells into anterior neural/mesodermal (A6.2, A6.4) and posterior endoderm (A6.2, A6.3) territories. At this stage nuclear β-catenin is restricted to posterior endodermal precursor cells (Figure 1A). The combined activities of FoxD, FoxA, and FGF signaling are both necessary and sufficient to create a Notochord/Neural state at the 32-cell stage characterized by *Zicl* expression, while these genes together with nuclear β-catenin activate the earliest endoderm specific gene, *Lhx3* (Hudson et al., 2013; Hudson et al., 2016).

Distinguishing notochord and neural fates requires differential MAPK activity (Figure 1A). Although it had been originally supposed that the notochord is able to form autonomously, Nishida (1992) found that continuous dissociation of blastomeres prevented cells from adopting a notochord fate, suggesting a requirement for inductive interactions during cleavage stages. Later it was shown that vegetal endodermal cells could be the source of this inductive signal (Nakatani and Nishida, 1994), and that the signal consists of FGF acting through the MAPK/Ets pathway (Kim and Nishida, 2001; Matsumoto et al., 2007; Nakatani and Nishida, 1997; Yasuo and Hudson, 2007). Despite these results, FGF is broadly expressed on the vegetal side of the embryo, making it surprising that FGF could act locally to generate differential MAPK activity among notochord and neural precursors. This led Picco and colleagues (2007) to look for an opposing signal coming from animal blastomeres which contact A-line neural cells

anteriorly. They found that ephrin expressed in a-line cells aids in the downregulation of MAPK activity in neural-precursors, mediated by P120RasGap (Haupaix et al., 2013). Zicl also plays a role in distinguishing notochord and neural fates. Its expression in notochord-neural precursors at the 32-cell stage is required for subsequent activation of the neural specific gene *FoxB* and the notochord specific genes *Brachyury* and *Mnx* (Hashimoto et al., 2011). MAPK signaling inhibits *FoxB* and activates *Brachyury*, while FoxB prevents *Brachyury* from being expressed in neural cells, locking in this binary cell fate decision.

Subdivision of the A-line neural lineage begins around the 44-cell stage, when a lateral Nodal signal originating from b6.5 activates expression of lateral specific genes in A7.8 (Figure 2). This signal was discovered by Hudson and Yasuo (2005) who showed that ablation of b6.5 leads A7.8 to lose expression of the lateral markers *Snail* and *Delta2* and ectopically express the medial marker *Otx*. This led them to investigate the impacts of Nodal, which is expressed in the b6.5 lineage (Imai et al., 2004). In their experiments, Nodal proved necessary and sufficient to induce lateral genes and repress medial ones. This includes markers from the 110-cell stage onwards, suggesting that Nodal is responsible for specification of lateral neural fates which persist even in the absence of continued exposure to Nodal. Indeed, a later study showed that lateral specification by Nodal acts before the 64-cell stage after which inhibition of this signal has no effect (Hudson et al., 2007).

Although Nodal signaling is able to distinguish A7.4 from A7.8, it is not capable of delimitating each of the 8 columns of A-line neural cells present from the 110-cell stage onwards. This distinction is mediated by delta signaling. Initially delta originating from the b6.5 lineage specifies the lateral-most column of cells and is required for the expression of genes such as *Neruogenin* and *HesB* in these cells (Hudson et al., 2007; Figure 2). This Delta signal is also required for expression of genes limited to A8.16 derivatives after they divide into A9.31 and A9.32. Because Nodal induces *Delta* in lateral A8.15 and A8.16 cells, this allows a second Delta signal to distinguish the identity of the 2 medial most columns (Figure 2). Specifically, exposure to Delta leads to inhibition of *FoxB* in A9.16, limiting this gene to A9.14. As a result of these two signals, each of the four A-line columns has experienced a unique combination of signals; (+) Nodal (+/-Delta) laterally and (-) Nodal, (+/-) Delta medially.

FGF signaling is deployed to distinguish between rows I and II of the posterior neural plate. In the absence of FGF, row I cells adopt the identity of their row II counterparts without losing their medial-lateral context (Hudson et al., 2007). Thus it appears that a combination of Nodal, Delta and FGF/MAPK signaling provides unique identities to each cell of the A-line neural plate at the mid-gastrula stage. Moreover, as discussed above, the steps leading to these identities have been determined from the first cleavage of the egg up until this point. Among the various animals used to study embryonic development, few lineages have been studied in such exquisite detail. Accordingly, the A-line neural lineage is an ideal system to study the consequences of specification on the subsequent morphogenetic behavior of cells.

Specification and Morphogenesis

During ascidian development, neurulation begins immediately after gastrulation. Morphogenesis of the neural tube is highly stereotyped with different cells adopting distinct behaviors during this process as described in chapter 3. A reasonable hypothesis is that the specification events giving identities to the cells of the neural plate are both necessary and sufficient to trigger the cellular behaviors required for morphogenesis. This does not rule out additional interactions between the cells as neurulation proceeds, but rather describes a situation where specification of the various identities within the posterior neural plate may be sufficient for morphogenesis to proceed autonomously among the cells of this group. In testing this hypothesis with a combination of live-imaging and lineage specific genetic perturbations, I have found that FGF/MAPK signaling is necessary and sufficient for intercalation movements of the ventral neural tube precursors, while Nodal is required for stacking movements of lateral cells.

This hypothesis fits nicely into an overall framework of embryonic development where iterative interactions between cells continuously refine cellular identity and behavior. In this scenario, the genetic basis of development can be attributed to the genome providing the correct instructions at each time point to each cell, such that cells respond to their environment in the appropriate way. How a cell interprets the genome is determined by its current molecular composition and external interactions which in turn stem from earlier sets of genomic instructions and their consequences. Given that the complement of all metazoan genes can be expressed in nearly limitless combinations (especially when taking into account different expression levels) it becomes clear that evolution is capable of tailoring the expression of these genes to every situation that a cell might encounter during development.

The way forward for developmental biology is therefore to continue developing our understanding of how each of these instructions is encoded in the genome along with how a cell will behave after reading out its instructions. Achieving this goal will require numerous model developmental processes from which we can eventually hope to understand whatever universal principals apply. My work is just a small but necessary step forward for one particular process. My hope is that it will serve as a milestone for future researchers using ascidian neural tube morphogenesis as a way of probing how is anatomy is encoded in the genome.

Figure 1

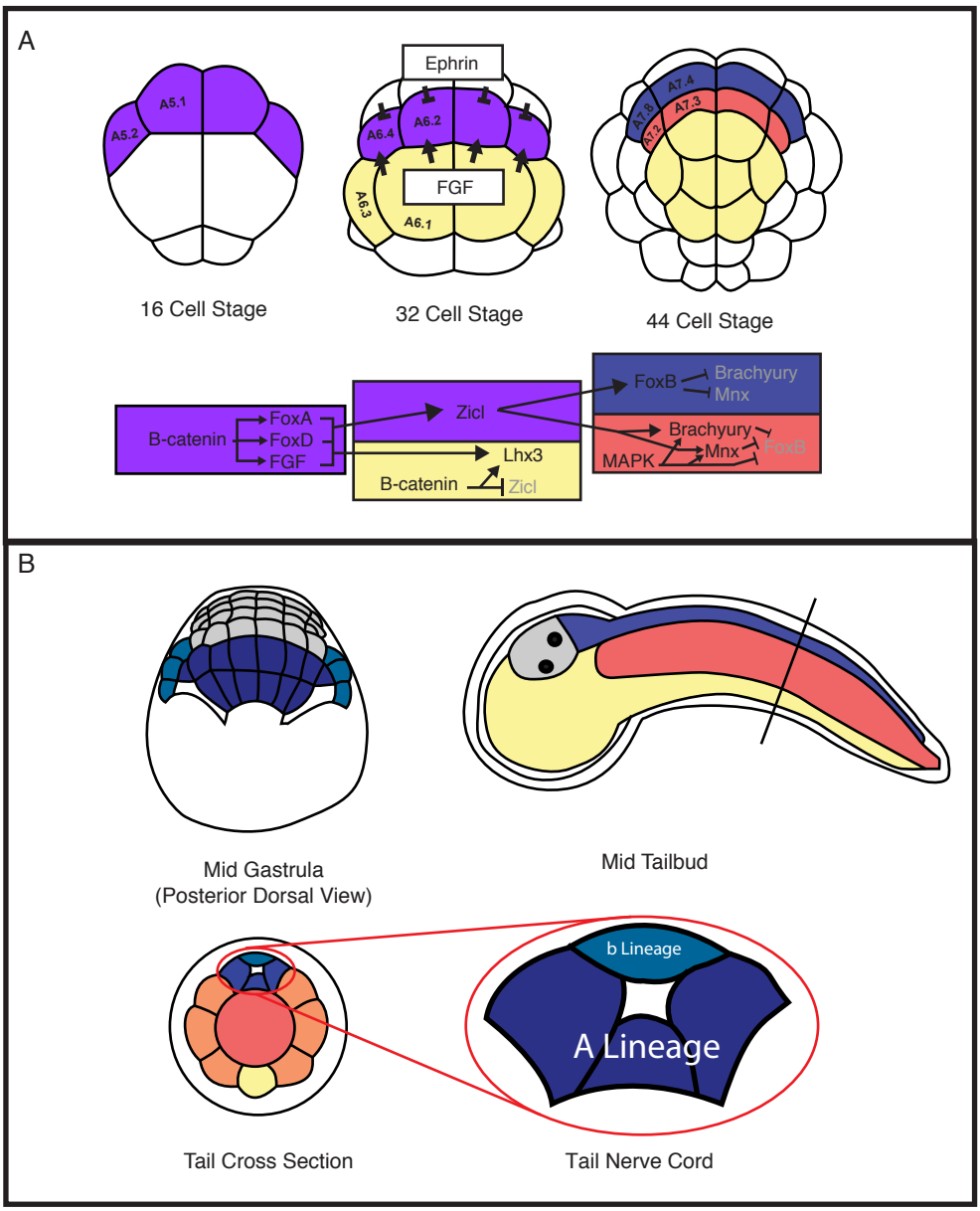

Ciona A-line neural development. (A) Segregation and specification of A-line neural fate. Top row: cartoons of embryos from the 16-cell stage through 44-cell stage. A-lineage is colored with unspecified cells colored purple, endoderm fated cells in red and neural fated cells in blue. At the 32-cell stage FGF emanating from vegetal blastomeres promotes MAPK activity in notochord precursors while ephrin signaling from a-line cells inhibits MAPK in A-line neural cells at the 44-cell stage. Bottom row: Key components of the A-line gene regulatory network. (B) Tail nerve cord lineages at mid-gastrula and mid-tailbud stages. Dark blue cells represent A-lineage which contributes to the ventral and lateral nerve cord, while light blue represents b-line cells contributing to the dorsal nerve cord. Gray represents a-line neural cells at the mid-gastrula stage and the a-line derived anterior sensory vesicle in tailbud embryo. Other tissues in tailbud cartoon are notochord (red), muscle (orange), endoderm (yellow) and epidermis (white). Lateral view of tailbud is a mid-sagittal section. Black bar shows location of tail cross section.

Figure 2

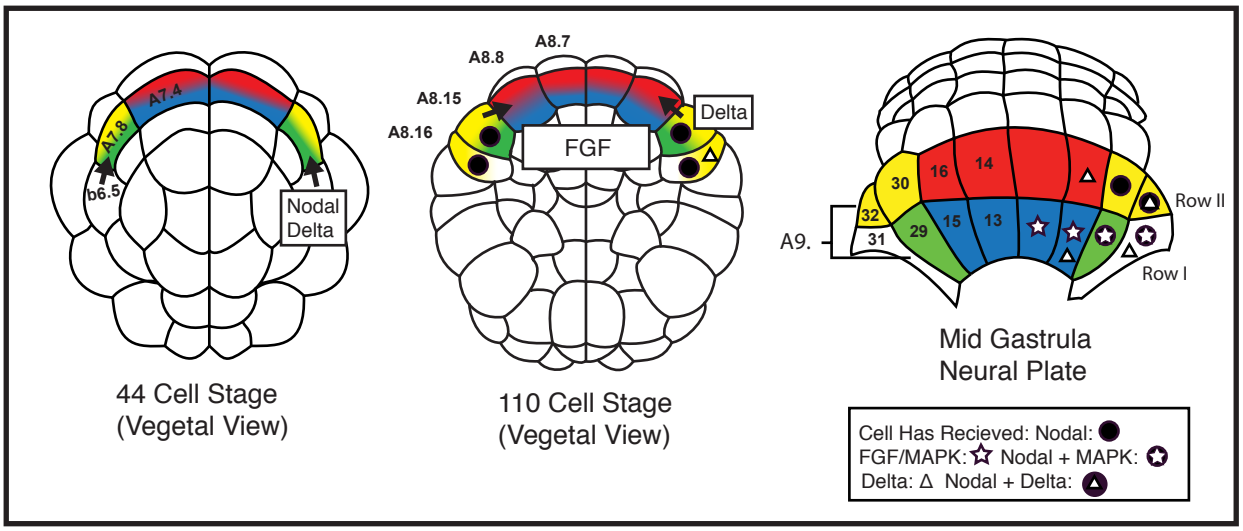

Specification of A-line neural cells by Nodal, Delta, and FGF signals. Left side blastomeres are labeled according to ascidian nomenclature. Colors represent cell lineages while symbols represent signaling according to legend. A9.31 contributes to the tail muscles and is therefore uncolored. At the 44-cell stage Nodal originating from the b6.5 blastomere signals to A7.8 but not A7.4, while Delta also originating from b6.5 impacts gene expression in A8.16 and its derivatives. At the 110-cell stage an FGF signal of unknown origin is transduced ultimately leading to MAPK activation in row I but not row II at the mid-gastrula stage. Delta emanating from A8.15 modulates gene expression in A8.8 derivatives.

Chapter 2: Materials and Methods

Molecular cloning

FoxB, *Snail*, *DMRT*, and *ETR* regulatory sequences have been reported previously (Corbo et al., 1997; Veeman et al., 2010; Wagner and Levine, 2012). The *Mnx* -5kb regulatory sequence was amplified from genomic DNA using the primers F-tatggcgcgcctcctgatg-tgacggatttatgactg, R-tatgcggccgctagcatcattttaaatcttaaatatcaaaggttc and cloned into a H2B:Cherry-containing expression vector using NotI and AscI restriction sites. The *Unc4*-3kb enhancer was similarly amplified using F- tatggcgcgccttggtggctaacgataacaacct-tc, R- tatgcggccgcattcatatttcaagtcgcaaaatagaaaagc and cloned using NotI and AscI sites. dnFGFR and Elk:VP64 were digested from Dmrt4>dnFGFR (Wagner and Levine, 2012) and Zicl>ElkLVP64 (Gainous et al., 2014) using NotI and BlpI and cloned downstream of the *FoxB* and *Mnx* enhancers. A clone of the *Ciona* MEK1/2 gene (citb42j03) was modified to produce the amino acid changes S116D and S220E using the primers tatgatcttgtccctacaaactcgttggccatatcgtcgatcagttgcccgctcac, gtgagcgggcaactgatcg-acgatatggccaacgagtttgtagggacaagatcata and the Stratagene quick-change site directed mutagenesis procedure. The modified coding sequence was then amplified using the primers F-tatgcggccgcgatgcctcctaaacgtaagttaa-acc, R-tatgaattcttaat-caggtacagtgtctggact and cloned into a vector containing the *FoxB* enhancer using NotI and EcoRI restriction sites. FoxD>Lefty and FoxD>Nodal (Mita and Fujiwara, 2007) were generously obtained from Shigeki Fujiwara. To construct Etr>Lefty, the Lefty coding sequence was amplified with F-tatgcggccgcgatggcccgggcgaa and R-ggatttccttacgcgaaatacg, digested with NotI/EcoRI and cloned into a vector containing the Etr enhancer.

Embryo manipulation

Adult wild caught *Ciona intestinalis* (species type A, 'robusta') animals were obtained from M-REP in San Diego, California. Protocols for fertilization, dechorionation and electroporation have been described (Christiaen et al., 2009b; Christiaen et al., 2009c). Plasmid concentration for electroporation varied between 15 and 50 μg per plasmid. For experiments with fixed embryos, healthy embryos were hand-chosen during gastrulation using glass pipettes stretched and broken to create a ~.5mm opening and a 10ml geared pipette pump. Embryos were subsequently fixed at the appropriate stage for analysis of neurulation phenotypes. For drug treatments both UO126 (Promega) and aphidicolin (Promega) were resuspended in DMSO and diluted to 10 μM in filtered artificial seawater (FASW). Embryos were fixed in MEM-FA (3.7% formaldehyde, 0.1M MOPS pH7.4, 0.5M NaCl, 1 mM EGTA, 2 mM MgSO4, 0.05% Triton X-100) for 20 min at room temperature, and then washed several times in PBTT (PBS+50mM NH4Cl+0.3% Triton X-100) and PBTr (PBS + 0.01% Triton X-100). For phalloidin staining, embryos were incubated overnight at 4º C with Alexa Fluor 488-conjugated phalloidin (Molecular Probes; 1:500) in PBTr, and then rinsed with PBS + 0.005% Triton X-100. Embryos were then equilibrated in 50% glycerol in PBS with 2% DABCO and left to settle in a glass coverslip bottom dish allowing them to be manually oriented prior to imaging. Only embryos exhibiting non-mosaic expression of reporter genes in A-line neural cells were included in analyses. Imaging was performed on inverted Zeiss 700 and 780 laser scanning confocal microscopes.

Time-Lapse live imaging and cell tracing

For live, time-lapse experiments embryos were reared in filtered artificial sea water and imaged on glass coverslip bottom dishes at 60 second intervals. Only experiments with good overall embryo health were included in our analysis, though some issues were tolerated particularly minor DNA bridging between cells which frequently occurred during cell division and seemed to be a largely unavoidable consequence of the electroporation/histone reporter/laser scanning confocal live imaging experimental scheme. Supplementary Table 1 shows the outcome of time lapse experiments performed for this project. Occasionally embryos drifted and had to be repositioned. Confocal slices were taken at 1.5μm intervals through the developing CNS from the dorsal side. The Fiji Trackmate plugin (Schindelin et al., 2012) was used to manually track cells and generate lineage trees and labeled movies. In cases where tracking was straightforward a maximum projection was generated prior to labeling cells, while in other cases cells were labeled on a slice by slice basis and a maximum projection was later created for display purposes.

Quantification of 11th generation cells

To quantify the number of 11th generation A9.14 and A9.13 derivatives, FoxB>H2B:Cherry electroporated embryos were fixed at the mid-neurula stage and stained with phalloidin. By carefully counting the total number of A-line neural cells present and examining their relative positions we were able to determine how many A9.14/13 derived cells were present in each embryo, and thus infer the number of 11th generation cells.

Membrane length analysis

Confocal microscopy was used to image a total of 90 non-mosaic embryos (46 controls and 44 expressing FoxB>caMEK) from 4 independent experiments. In each experiment healthy LacZ and caMEK electroporated embryos were collected prior to the late gastrula stage at which point some embryos from each group were treated with aphidcolin to prevent A-line cells from reaching the 11th generation. Embryos were then fixed at the mid-neurula stage. Before imaging, embryos were manually oriented such that their dorsal side faced the objective and a confocal stack through neurulating cells was acquired at <1μm intervals. For embryos treated with aphidicolin a slice best representing the midway point between apical and basal surfaces of A9.14 derived cells was then chosen for each embryo. We then used image J to trace the phalloidin membrane staining on this slice starting from the midline where a-line derivatives intersect A9.14 derived cells anteriorly and ending at the midline where A9.14 cells intersect A9.13 derivatives. The image J 'measure' command was used to calculate the length of the traced membrane. In cases where the shortest span was ambiguous both were measured and the shorter possible span was used. A p-value comparing lacz+aphidicolin and caMEK+aphidicolin membrane lengths was calculated using the Wilcoxon two-sample test and boxplots were generated using BoxPlotR web tool. Embryos where cell identity was ambiguous or an A9.14 derived cell had entered the 11th generation despite aphidicolin treatment were excluded from the membrane length analysis.

Chapter 3: A-Line Neural Tube Morphogenesis

Introduction

Molecular phylogenetic evidence suggests that tunicates such as *Ciona* are the closest living relatives of vertebrates (Delsuc et al., 2006). Indeed, the CNS of the ascidian tadpole has the same basic organization as that of vertebrates. It includes a sensory vesicle (simple brain) and nerve cord corresponding to the vertebrate spinal cord (Lemaire et al., 2002). Nevertheless, it is highly simplified, with just ~330 cells comprising the CNS in mature larvae (Nicol and Meinertzhagen, 1991). In addition to its small cell number, *Ciona*'s fixed patterns of cleavage and invariant lineages (Conklin, 1905; Nishida, 1986) provide opportunities for understanding how individual cellular behaviors contribute to morphogenetic processes, such as formation of the neural tube.

Morphogenesis of the ascidian CNS follows a similar profile to that observed in vertebrate embryos (Nicol and Meinertzhagen, 1988a). During gastrulation, CNS progenitors come to occupy a flat neural plate on the dorsal side of the embryo. Neural tube formation (neurulation) begins immediately after the completion of gastrulation. Apical constriction causes bending of the neural plate, while a combination of oriented cell divisions and convergent extension movements results in a lengthening of the plate. Eventually, the lateral plate borders, aided by force from the surrounding epidermis (Ogura et al., 2011), meet at the dorsal midline together with the adjacent epidermis. Sequential contractions and rearrangements of neural-epidermal junctions cause a progressive posterior to anterior fusion of the epidermis overlying the neural tube following involution (Hashimoto et al., 2015).

The quest to trace the cells of the ascidian central nervous system dates back to the late 19th century when embryologists such as Alexander Kowalevsky, Laurent Chabry, and Ernest Castle worked to directly observe and describe ascidian development. Early work in this area culminated with Edwin Conklin's 1902 cell lineage study, where he successfully traced cells from the first cleavage up until the mid-gastrula stage, with its 6 rows of ninth generation neural precursors. He was also able to determine that the anterior CNS is derived form the a-lineage while the posterior nerve cord is derived from "those neural plate cells which belong to the dorsal hemisphere and which in origin are intimately associated with the chorda cells," i.e. the A-line neural cell lineage.

Subsequent attempts to trace the fate of neural progenitors beyond the stage where they can be directly observed can be divided into two categories based on the approach used. The first of these is studies that use a lineage tracer to mark cells at an early stage when they are easily identified, and then look at where the marked cells end up in later stages. The second approach involves collecting embryos at each stage of development and progressively assigning cells to a given lineage based on the locations of cells at the previous stage.

The use of intracellular lineage tracer in ascidian embryos was pioneered by Hiroki Nishida, who sought to test Conklin's assertion that each cell at the 64-cell stage contributes to just a single tissue (Nishida, 1987). Injecting each blastomere at the 64-cell

stage, Nishida found that this is not the case. Among the exceptions is the A-line neural lineage, which he showed gives rise not just to neural precursors, but also muscle cells. As part of this study, Nishida injected each of the 8th generation A-line neural blastomeres to determine where descendants of these cells ended up at the mid-tailbud stage. He found that A-line neural cells contribute to the ventral and lateral portions of the nerve cord and posterior portions of the brain (the "brain stem"). A further study using lineage tracer has extended our knowledge of neural fates to the larval stage (Taniguchi and Nishida, 2004).

The gold standard for ascidian neural cell lineages has been the works of Nicol and Meinertzhagen (1988a, 1988b) and Cole and Meinertzhagen (2004). These studies traced each cell by carefully analyzing embryos fixed at successive stages, providing information not only about the ultimate fate of each cell, but also the shape changes, movements, and patterns of division along the way. The earlier study used serial sections to reconstruct cell maps for embryos collected every 12 minutes. Transverse sections provide information on cell shape changes, while cell-surface reconstructions portray the relative movements of cells. Cole and Meinertzhagen's 2004 study extended this analysis to later stages, using confocal microscopy to examine the locations of nuclei as the nervous system forms.

Despite the accomplishments of these earlier works, a functional study of neurulation requires a rapid and comprehensive way of assessing neural tube morphogenesis that can be repeated for a variety of conditions. For this reason we turned to time-lapse live imaging, which combines the best features of lineage tracing (unambiguous marking of target cells) and analysis at successive stages, in this case separated by only a minute. Combining time lapse experiments with analysis of fixed embryos resulted in a detailed look at the lineages and movements of A-line neural cells during neurulation, and revealed a number of important deviations from previously published work.

Results

To explore how cells of the posterior CNS move and divide during neurulation we used time-lapse confocal microscopy to visualize the nuclei of these cells starting at the mid-gastrula stage. Nuclei were labeled by electroporation of a FoxB>H2B:YFP reporter gene (Imai et al., 2009), which recapitulates endogenous *FoxB* expression in A7.4, A7.6 and A7.8, and later in the lateral epidermis during neurulation (Imai et al., 2004, Figure 3). In a control embryo co-electroporated with FoxB>H2B:YFP and FoxB>LacZ, we traced cells until the mid-tailbud stage (Figures 4A-D,I; Figure 5; Figure 6). The results obtained were consistent with those from other time-lapse experiments (Table 1), including experiments where a membrane localized YFP-CAAX reporter was used to visualize cell shape changes during neurulation (Figure 7).

The most important finding of our experiments is that A-line neural cells have three distinct behaviors during neurulation, and that the cells undergoing each behavior are already segregated at the mid-gastrula stage. Medial row II cells undergo an early oriented division to enter the 11th generation but otherwise remain in place. Meanwhile, medial row I cells converge at the midline and intercalate such that 10th generation sister

cells lose contact. Finally, lateral cells of both rows participate in a process we call "lateral stacking," in which cells rearrange to form a single anterior-posterior oriented stack, but retain contact with 10th generation sisters. The details of A-line neurulation movements are described below, followed by a discussion of cases where our results deviate from previous interpretations.

Lineage and movements of the A-line neural progenitors

At the beginning of gastrulation, the A-line neural lineage consists of a single row of eight blastomeres aligned medio-laterally (Figure 2). At this stage the embryo is bilaterally symmetric and so there are four A-line neural blastomeres on each side of the embryo, consisting of two lateral derivatives of A7.8 (A8.16 and A8.15) and two medial derivatives of A7.4 (A8.8 and A8.7). As gastrulation proceeds this row of cells comes to occupy the dorsal rim of the blastopore. During the transition from early to mid-gastrula, each cell divides in an anterior-posterior orientation to create the two posterior-most rows of the neural plate. In the two time-lapse movies which capture this division, it appears that lateral cells complete this division just before medial ones, but all cells divide within a ~15 minute period (Figure 7). As a consequence of this division, and continued gastrulation movements, medial cells form a grid just anterior to the blastopore, while lateral cells shift posteriorly, with A9.29 initially occupying a position between A9.30 and A9.31, and underneath A9.32.

As gastrulation continues, the blastopore becomes smaller. A-line cells in contact with the blastopore become pinched on the side facing the blastopore, resulting in a semi-circular configuration (Figure 7). As development proceeds into the late-gastrula stage, A-line neural cells exhibit asynchronous cycles of division that can be assigned to different groups based on timing (Nicol and Meinertzhagen, 1988b). Cells within a group enter and exit mitosis within a ~15 minute time window that is distinct from cells in earlier or later dividing groups. The first group of cells to divide is A9.16 and A9.14 belonging to medial row II. This is followed by medial row I cells (A9.15 and A9.13) and the lateral cells A9.29 and A9.32; A9.30 is the last to divide (Figure 5).

Reorganization of neural progenitors into the lateral and ventral regions of the future neural tube also begins at the mid-gastrula stage (Figure 4, see also Figure 15). The lateral walls of the tube are initially formed by the posterior movements of A9.30, A9.29, and A9.32 derivatives relative to A9.16 derived cells; we will refer to this collective set of movements as "lateral stacking." During the transition from mid to late gastrula, A9.29 moves posterior to A9.30 and underneath A9.32, separating these cells. Simultaneously, A9.30 begins to slide behind A9.16, a movement which is not completed until both cells have divided. Finally, derivatives of A9.32 eventually move posterior to A9.29 progeny. Each 10th generation lateral cell remains in contact with its sister cell, resulting in a pair of lateral stacks that extend from anterior to posterior regions of the neural plate at the early neurula stage (Figure 4B,F). To form the ventral "floor plate" A9.13 and A9.15 derivatives converge at the midline, intercalate and separate from their sisters (Figures 4, 6A). In most cases three of the four A9.13 derivatives intercalate at the anterior end of the floor plate, while the fourth cell ends up between left and right pairs of A9.15 derivatives, which remain on either side of the midline through the mid-neurula stage. The anterior-

most floor plate cell arises from the left A10.26 blastomere in some embryos, and the right A10.26 cell in others (Table 1). These movements are consistent with those described by Nicol and Meinertzhagen (1988a).

The transition from early to mid-neurula is characterized by the continued intercalation of the floor plate and the entry of medial row II (A9.14 and A9.16) derivatives into the 11th generation (Figure 4C,G). A9.14 derivatives divide first, followed by the anterior A9.16 derivative (A10.32) and finally the posterior A9.16 derivative (A10.31), though all cells divide within the same ~20 minute period. The results is an anterior-posterior oriented group of four A9.14 derived cells located anterior to the floor plate on either side of the midline, and a similar group of A9.16 derivatives anterior to the rest of the lateral cells on each side (Figure 4C,G). At this point A9.16 derivatives have shifted backwards so that the anterior-most cell (A11.64) is adjacent to the posterior-most A9.14 derivative (A11.53).

As A10.31 finishes dividing, many of the remaining A-line neural cells begin entering the 11th generation (Figures 4D,E; 6). First are derivatives of A9.29, which divide more or less simultaneously. This is followed by A10.60 and then A10.59. Floor plate cells also begin entering the 11th generation at this stage, with the anterior most cells dividing last. At this time floor plate cells also begin to extend anteriorly between left and right A9.14 derivatives, which until this point have been in contact on either side of the midline. A9.16 derivatives bulge outwards, which may help A9.14 derived cells move in front of A9.16 cells to form the anterior-most portion of the A-line derived lateral neural tube. Meanwhile, A10.64, which does not divide again, leaves the lateral neural tube and beings to migrate anteriorly along the tube's side. A10.63 remains at the posterior end of the tube, but does not yet divide. At this point the embryo is at the late-neurula stage.

The main morphogenetic event during the transition to the initial tailbud stage is the final intercalation of 11th generation A9.15 derived floor plate cells, such that the floor plate now consists of a single file line of ventral cells. Other cells maintain their relative positions as the embryo elongates. During the transition from initial to early tailbud stages, A9.14 derivatives divide in a dorsal-ventral orientation to enter the 12th generation, thus beginning formation of the A-line derived portion of the sensory vesicle. Behind these cells, A9.16 derivatives enter the 12th generation dividing again in an anterior-posterior orientation. These cells divide in a characteristic sequence, with A11.64 dividing first, followed by A11.63 and A11.61. Division of A11.62 is significantly delayed, and does not occur until the mid-tailbud stage. Meanwhile, 11th generation A9.29 derivatives begin to enter the 12th generation, dividing in sequence starting with the posterior-most cell (A11.113). A10.63, still occupying the posterior-most position of the lateral tube walls, also divides (Figure 6).

The final divisions we were able to trace via time-lapse occurred during the mid-tailbud stage (Figure 4I, J). Among A9.30 derivatives, A11.119 divides first, followed by its sister, A11.120. The A9.16 derived cell A11.162 also divides around this time. At this point A10.64 has migrated anteriorly along the tail, to a point just posterior to the A9.30 derivatives that eventually make up the trunk ganglion. The lateral portion of the A-line

derived CNS at this stage from anterior to posterior thus consists of four sets of dorsal-ventral oriented cell pairs derived from A9.14, followed by eight cells derived from A9.16, six A9.30 derivatives of the future trunk ganglion, eight A9.29 derivatives while are likely future ependymal cells, and finally two cells derived from A9.32 (Figure 4I,J). The ventral A-line derived floor plate, which spans the entire length of this portion of the neural tube, consists of a 25 cells in a single file line. At this stage the floor plate is mixture of 11^{th} and 12^{th} generation cells.

Comparing the cell positions from our time lapse experiments to the 3D virtual tadpole (Nakamura et al., 2012), a reconstruction of all cells at a slightly later point during the mid-tailbud period, it became apparent that the anterior-most A-line derived cells likely make a second dorsal-ventral oriented division to create the walls of the "middle sensory vesicle" which consists of four rows of four cells each. To confirm this suspicion, we electroporated embryos with a combination of FoxB and DMRT reporters, which mark the A-line and a-line neural lineages respectively (Figure 8). These experiments clearly revealed an A-line derived portion of the sensory vesicle matching the configuration of the "middle sensory vesicle," suggesting that these cells are derived from the A- rather than the a-lineage (Cole and Meinertzhagen, 2004; Nakamura et al., 2012).

Revised lineage of A-line neural cells

Time-lapse live imaging revealed that the organization of A-line cells during neurulation is simpler than previously thought. Especially striking is the observation that the floor plate is derived entirely from A9.13 and A9.15, while A9.14 contributes only to the sensory vesicle. It seems probable that A9.14 gives rise to the lateral portions of the "middle sensory vesicle" identified by Nakamura et al. (2012), which is consistent with studies showing that the photoreceptors of the ocellus are derived from the medial A-lineage (Gainous et al., 2014; Oonuma et al., 2016; Taniguchi and Nishida, 2004). It therefore appears that the basic subdivision of the posterior CNS into middle sensory vesicle, posterior sensory vesicle, trunk ganglion, lateral spinal cord, and floor plate is already established at the mid-gastrula stage, similar to the time when CNS patterning becomes evident in vertebrates (Lumsden and Krumlauf, 1996).

Our live imaging studies suggest that the precise order of medial convergence in the floor plate may not be fixed, but is somewhat variable among different embryos. Similar variability is observed for the intercalation of the notochord during the convergence of left and right progenitors across the midline (Miyamoto and Crowther, 1985; Nishida, 1987). We are also curious about the final fate of A10.64 cells, which migrate anteriorly along the neural tube as the tail extends. It is conceivable that these cells respond to the same migratory cues as BTN cells which possess some of the properties of neural crest derivatives (Stolfi et al., 2015). It is also possible that A10.64 cells correspond to the Islet-positive neurons of the trunk ganglion (Stolfi and Levine, 2011) rather than A10.57. Finally, A9.29 derivatives form most of the cells comprising the lateral neural tube posterior to the trunk ganglion, providing 8 cells on each side at the mid-tailbud stage.

As a results of our work, A-line neural cells can be definitively identified up to the mid-tailbud stage. Further work will be needed to determine the movements of cells beyond

this stage. Of particular interest is the rotation of the sensory vesicle (Taniguchi and Nishida, 2004) and the formation of neuronal processes and synapses within the nervous system prior to larval hatching. Overall, our work tracing A-line neural cells has provided a solid basis for our subsequent work linking specification and morphogenesis described in chapter 4, and we hope that it will be serve as a useful resource for future work on development of the A-line derived portions of the ascidian nervous system.

Figure 3

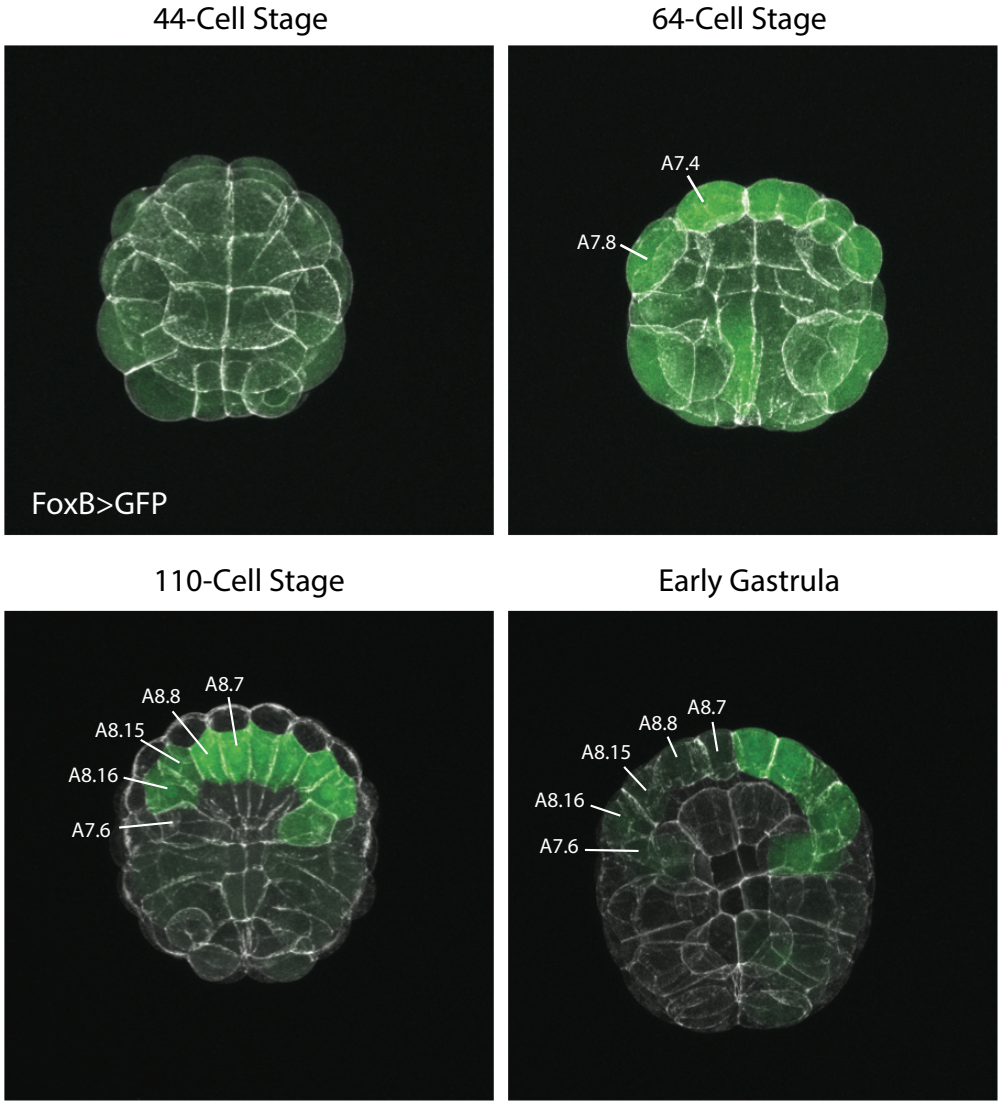

Early activity of FoxB enhancer. Maximum projection of embryos at the indicated stage showing FoxB>GFP expression in green and phalloidin staining in greyscale. Identities of reporter expressing cells are indicated on the left side of embryos. Early gastrula embryo is mosaic with limited expression on the left side.

Figure 4

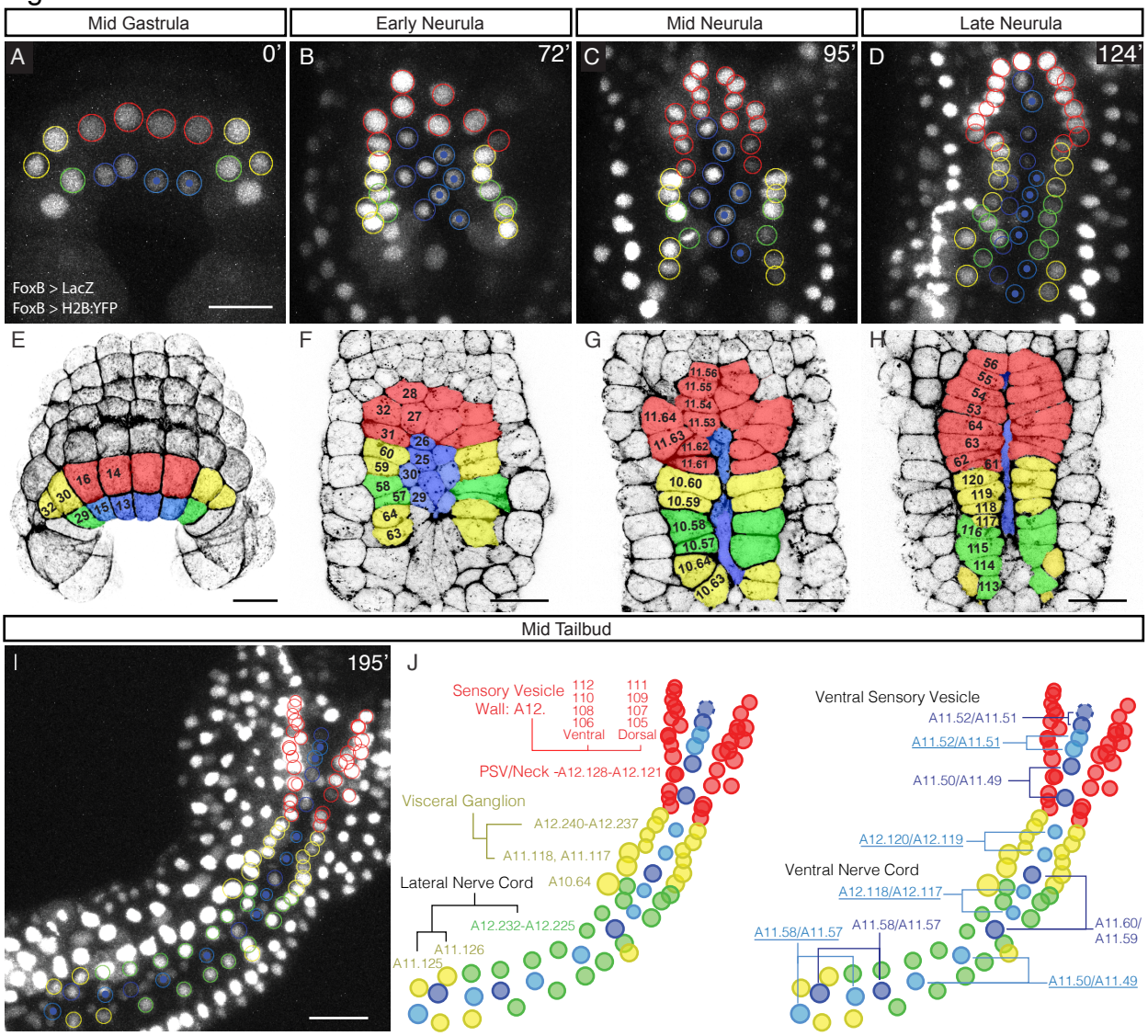

Revised A-line neural lineage. (A-D,I) Time lapse of embryo electroporated with FoxB>H2B:YFP and FoxB>LacZ from mid-gastrula stage to mid-tailbud stage. Circled cells belong to the A-line neural lineage. Cells were manually traced and labeled with FIJI trackmate plugin. Where cells from the left and right sides of the embryo mix, right side cells are indicated by a dot within the nucleus. (E-H) False colored images of phalloidin stained embryos labeled with cell identities corresponding to the cells tracked in (A-D). Embryos were electroporated with FoxB>H2B:Cherry to aid in cell identification and LacZ as a control for later experiments. (E) 3D projection of mid-gastrula stage embryo. Labeled cells are A-line of the 9th generation. (F-H) Single confocal slices from embryos at the indicated stages. (F) Labeled cells are of the 10th generation. (G) Labeled cells are of the indicated generation. (H) Labeled cells are of the 11th generation. (J) Identities of A-line neural cells tracked to the mid-tailbud stage. Dotted circle represents the presumed location of A11.52 which moves beyond stack depth at 182 minutes. The following deviations from the published fate map were observed in this and other time lapse experiments: A9.14 contributes to lateral walls (7/7), sixteen A9.29 derivatives at late neurula stage (6/6), anterior migration of A10.64 (3/3, unable continuously trace in other experiments). Underlined labels indicate cells derived from right side blastomeres. Colors reflect the lineage of each cell as in Fig. 1B. All scale bars are 25 μm.

Figure 5

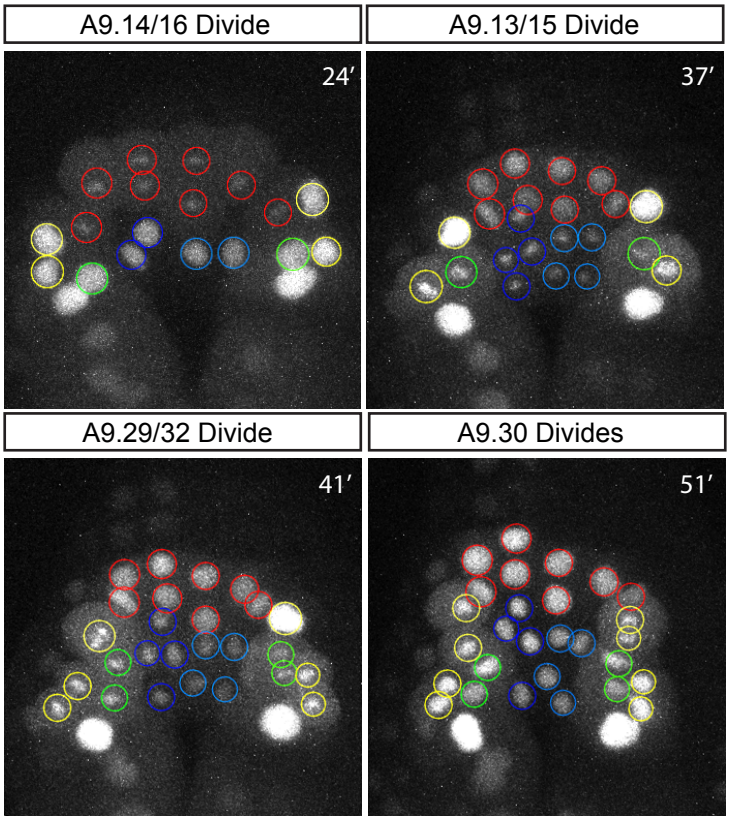

Timing of entry into the 10th generation. Stills from timelapse of FoxB>H2B:YFP and FoxB>LacZ electroporated embryo (Movie 1) showing A-line cells entering the 10th generation at the indicated time points. In control embryos medial row II cells always divide first (n=7/7) and A9.30 is always last (n=7/7).

Figure 6

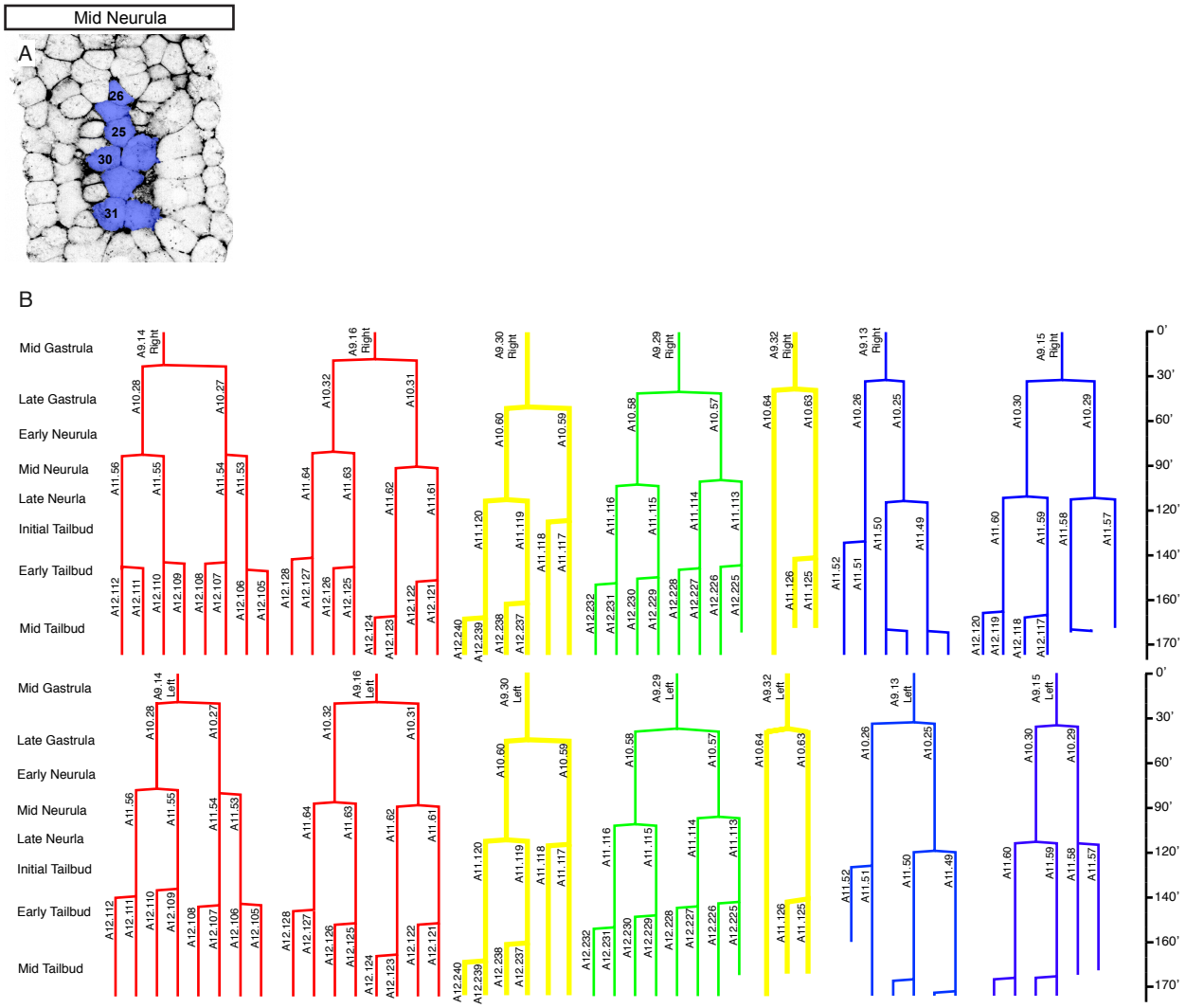

Division timing and lineage trees of A-line cells. (A) Confocal slice of embryo in Fig. 1G showing floor plate cells at the mid-neurula stage. (B) Lineage trees derived from movie 1 using the trackmate plugin. Stage is shown on the left and minutes into movie on the right.

Figure 7

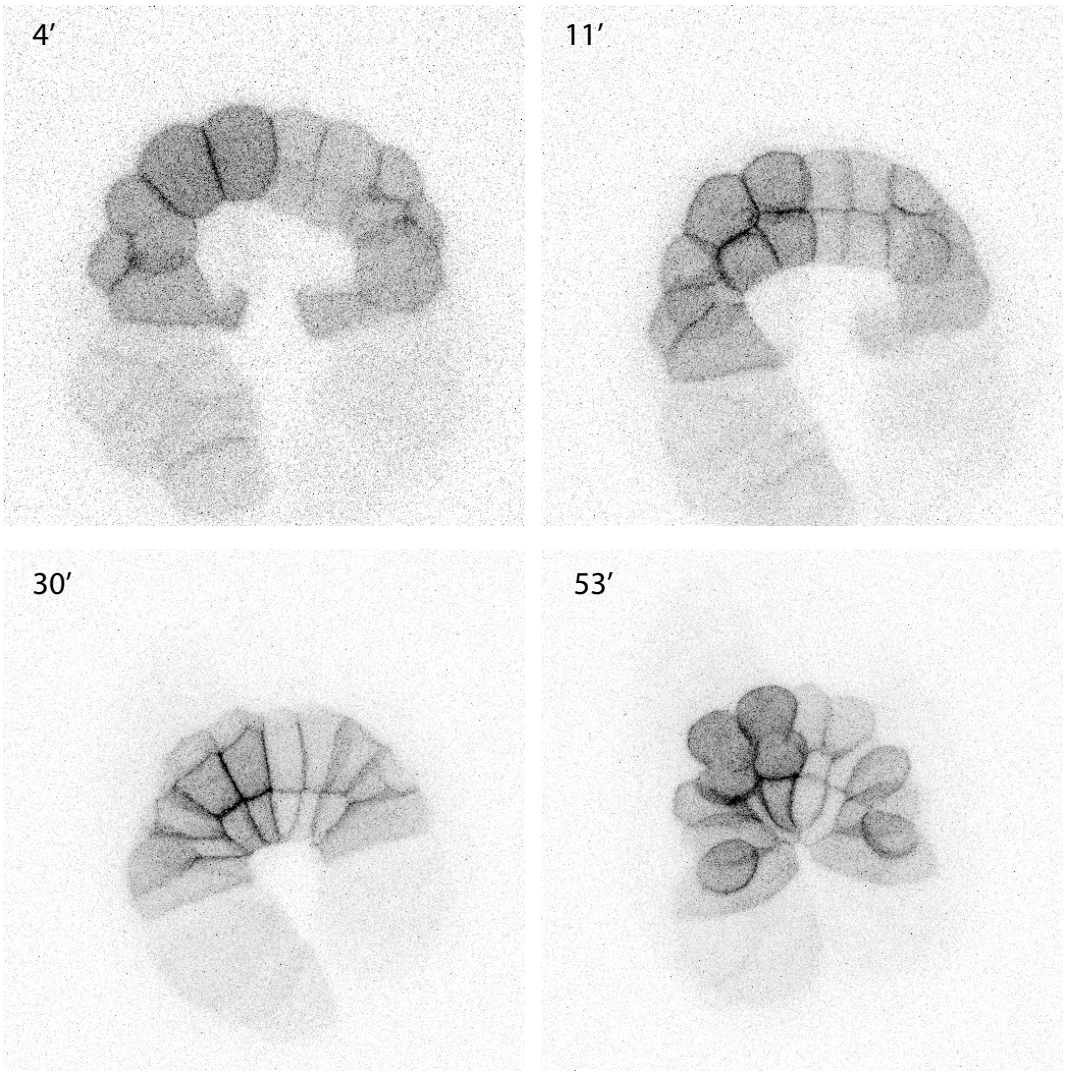

Transition from gastrula to neurula neural plate. Stills from time lapse of embryo electroporated with FoxB> YFP-CAAX at starting at the final moments of the early-gastrula stage.

Figure 8

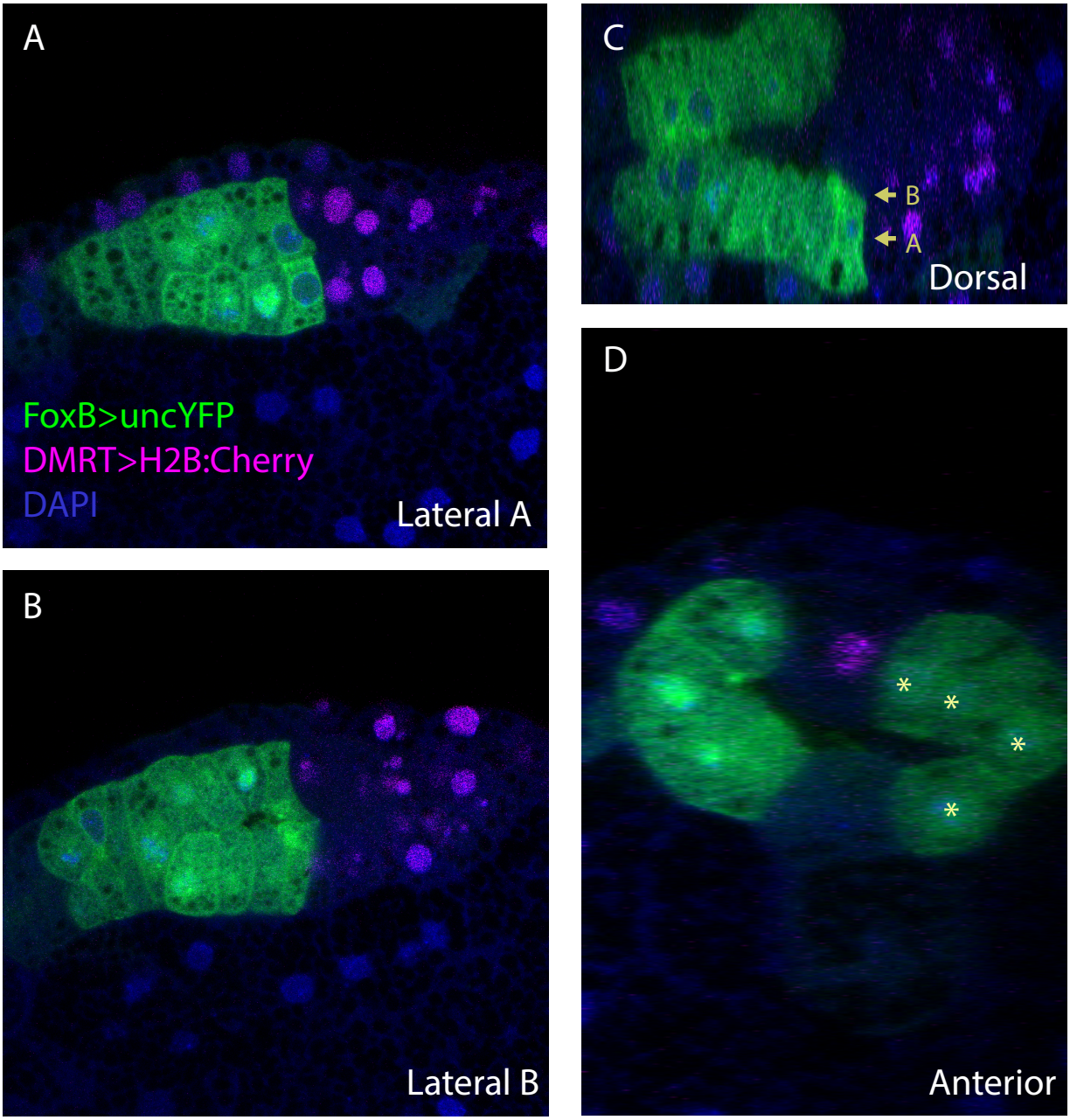

Middle sensory vesicle is derived from the A-lineage. Single confocal slices (A,B) and reconstructions (C,D) from mid-tailbud stage embryo electroporated with the indicated transgenes and stained with DAPI. Arrows indicate plane of lateral slices while asterisks indicate nuclei of FoxB (+) cells on one side of the sensory vesicle confirming that the middle sensory vesicle wall is comprised of four A-line derived cells at the mid-tailbud stage.

Chapter 4: Nodal and FGF Coordinate Ascidian Neurulation

Introduction

A central challenge in development is to understand how groups of cells self-organize into complex structures. It is generally assumed that cell specification events cause cells to express different sets of genes, which in turn determine their morphogenetic behaviors during development. Nevertheless, there are surprisingly few examples where cell specification has been directly linked to morphogenetic behaviors of individual cells (Ettensohn, 2013). Due to its simplicity, the ascidian central nervous system (CNS) offers an outstanding opportunity to connect specification and morphogenesis in the context of chordate embryogenesis. Here, we investigate the role of FGF and Nodal signaling in coordinating the early stages of neural tube morphogenesis in the ascidian *Ciona intestinalis.*

Our work is focused on the *Ciona* nerve cord. Considered in cross-section, it is composed of only 4 cells, including ventral and lateral ependymal cells that exhibit gene expression properties of the floor plate and lateral plate borders of the vertebrate neural tube, respectively (e.g., Corbo et al., 1997). These ventral and lateral cells are derived from the anterior vegetal (A-line) blastomeres (Figure 1B). A-line cells contributing to the neural tube are segregated at the 44-cell stage when lateral A7.8 and medial A7.4 cells separate from their sisters, which form the primary notochord lineage (Nishida, 1987). Around this time A7.8 receives a Nodal signal from lateral b6.5 blastomeres, resulting in the induction of *Snail* and the repression of medial identity (Figure 2; Hudson and Yasuo, 2005; Hudson et al., 2007; Hudson et al., 2015; Imai et al., 2006). Disruption of this signal causes neural tube defects and mis-expression of genes known to be involved in neural tube patterning and morphogenesis (Mita and Fujiwara, 2007; Mita et al., 2010).

Prior to gastrulation both A7.8 and A7.4 undergo a mediolateral division to create the row of 8 cells seen at the 110-cell stage (Figure 2). During gastrulation these cells divide again, this time along the anterior-posterior axis, to create rows I and II of the neural plate at the mid-gastrula stage. Before this division FGF induces subsequent activation of the MAP kinase (MAPK) signaling cascade in row I but not row II cells (Hudson et al., 2007). As a consequence of this differential MAPK activity, genes such as *Mnx* are activated only in row I, while others such as *FoxB* are restricted to row II (Hudson et al., 2007). Thus at the mid-gastrula stage combinatorial FGF and Nodal signaling provides distinct identities to A-line cells comprising the presumptive neural tube (Figure 2).

We employed a combination of time-lapse live imaging and lineage specific genetic perturbations to investigate how Nodal and FGF signals coordinate movements of lateral and ventral neural progenitor cells during neurulation. We find that FGF signaling is essential for intercalary movements leading to midline convergence of ventral “floor plate” cells. We also present evidence that Nodal signaling is required for proper stacking of lateral cells. In the absence of both FGF and Nodal signaling, neural progenitors exhibit a default behavior of sequential anterior-posterior oriented divisions. These results suggest a direct impact of FGF and Nodal on the cellular behaviors underlying neurulation.

Results

As described in chapter 3, the results of live imaging experiments demonstrate that there are three main behaviors among A-line neural progenitors during the early stages of neurulation, and that the cells undergoing each of these behaviors are segregated at the mid-gastrula stage. To test the hypothesis that the Nodal and FGF signals giving unique identities to these cells are also responsible for their morphogenetic behaviors we used live imaging to examine the consequences of perturbing these signals.

FGF is essential for midline convergence of A9.13 and A9.15 derivatives

FGF signaling distinguishes the identities of progenitor cells located in rows I and II of the neural plate (Hudson et al., 2007). Inhibition of FGF at the 110-cell stage causes row I cells to lose expression of row I markers and ectopically express genes normally restricted to row II. Given that ventral cells arise from row I, we sought to determine whether FGF is also required for the intercalary behavior of these cells. Towards this goal we selectively expressed a dominant negative form of the FGF receptor (dnFGFR) in the A-line neural plate using the FoxB enhancer. The consequences were examined in living embryos using time-lapse confocal microscopy (Figure 9A-C). We observed a number of changes relative to control embryos. First, all medial cells (A9.14, 16, 13 and 15) divided within the same 15-minute time window (Figure 9B; compare with Figure 5), and enter the 11^{th} generation before lateral cells. Second, derivatives of A9.13 and A9.15 fail to converge at the midline, and retain contacts with their sister cells (Figures 9C; 18C,D). Phalloidin staining of mutant embryos confirmed that A9.13 and A9.15 derivatives fail to intercalate, and instead line up on either side of the midline mimicking the normal behavior of A9.14 derivatives (Figure 9D-F). At the mid-neurula stage at least one daughter of A9.13 reached the 11th generation in 87% of all embryos examined, as compared with just 3% in control embryos (Figure 11H).

To test whether floor plate convergence requires FGF signaling beyond the initial specification of row I fates we inhibited signaling at the mid-gastrula stage. We began by using the MEK inhibitor UO126 to block MAPK signaling. As expected, treatment at the 110-cell stage caused intercalation defects consistent with the adoption of medial row II behaviors by A9.13 and A9.15 derivatives (Figure 9F). This treatment also seemed to cause a slight delay in overall development, which likely accounts for the reduction of precocious divisions observed relative to electroporation of FoxB>dnFGFR. In contrast, UO126 treatment at the mid-gastrula stage resulted in only occasional defects in the convergence of A9.13 and A9.15 derivatives, suggesting that the requirement for MAPK signaling is confined to specification at the 110-cell stage. To test for MAPK independent FGF signaling we expressed the dominant negative receptor using an Mnx enhancer active in A9.13 and A9.15 derivatives starting at the mid-gastrula stage (Figure 10). This caused convergence defects in more than 50% of embryos examined, suggesting that MAPK independent FGF signaling may play a continuing role in floor plate intercalation (Figure 9F).

We next sought to determine whether FGF signaling is sufficient to induce intercalary behaviors in medial row II cells, which normally form lateral regions of the sensory

vesicle. To do so we expressed a constitutively active form of the *Ciona* MEK kinase (Mansour et al. 1994) using the FoxB enhancer (Figure 10). Cell identities were monitored using the Mnx enhancer attached to a H2B:Cherry reporter. Misexpression of activated MEK caused ectopic activation of the Mnx reporter, consistent with a transformation of row II cells to row I identity (Figure 11E,F). Time-lapse imaging of mutant embryos revealed multiple changes in cell behavior. In contrast to control embryos (Figure 5), divisions of medial row II cells (A9.14/A9.16) occurred within the same 15-minute period as divisions of medial row I (A9.13/A9.15) (Fig. 5B). Furthermore, derivatives of A9.14/A9.16 did not enter the 11th generation prior to the mid-neurula stage (Figure 11C,H). Importantly, we also observed midline convergence of A9.14 derivatives, whereby sister cells lose their contacts during rearrangement (Figures 11C; 18E,F). This behavior is in stark contrast to control embryos where A9.14 derivatives remain confined to either side of the midline (e.g. Figure 4C,G, 11E). Midline convergence of A9.14 derivatives is clearly visualized in fixed embryos stained with phalloidin (Figure 11D,F).

We next asked whether FGF signaling induces ventral cell behaviors by transcriptionally regulating specific target genes. To do so we overexpressed a constitutively active form of the FGF/MAPK transcriptional effector, Elk:VP64, which is a member of Ets family of transcription factors (Gainous et al., 2014). Co-electroporation of embryos with a FoxB>Elk:VP64 transgene and Mnx>H2B:Cherry reporter resulted in ectopic expression of the Mnx reporter in A9.14 and A9.16 derivatives (Figure 11G), as seen with constitutive FGF signaling (Figure 11F). Ectopic expression was also observed at a lower frequency in other A-line neural cells. Changes in cell behaviors were also detected, including delays in division and midline convergence of A9.14 derivatives (Figure 11G,H), consistent with FGF mediating midline convergence via transcriptional targets.

It is possible that induction of midline convergence of row II cells is a passive response caused by the delay of cell division and surrounding forces in the embryo. To explore this possibility we used the DNA polymerase inhibitor aphidicolin to prevent row II cells from entering the 11^{th} generation, mimicking the delay in division caused by MAPK activation (Figure 12A). We then measured the length of membrane spanning the midline across row II derivatives, reasoning that a lengthening of this span will necessarily accompany convergence of cells across the midline (Figure 12C,D). Comparing aphidicolin treated embryos with and without MAPK activation, we found that MAPK activation induces midline convergence beyond any possible effects of delaying cell division alone (Figure 12B).

To better visualize midline convergence we used the FoxB enhancer to drive a membrane targeted YFP reporter gene (YFP-CAAX) (Figure 13A,B). We found that in both normal ventral cells (row I) and "activated" row II cells, midline rearrangements occur by contraction of localized junctions resulting in the separation of sister cells through neighbor exchange (also known as a T1 transition). Intercalation begins when mediolateral junctions spanning sister cells contract causing cells to the left and right sides to come into contact. The process is completed when an anterior-posterior oriented

junction is established between these cells. Two additional points are worth noting. First, 10th generation A9.14/16 derived cells transformed to a medial row I identity by MAPK activation are larger than row I cells, as is the case in unperturbed embryos (Nicol and Meinertzhagen, 1988a), suggesting a source of asymmetry not determined by MAPK signaling alone. Second, rearrangement of the converted cells takes longer than that of normal row I cells.

Nodal is required for lateral stacking

Perturbing FGF signaling had no apparent impact on the stacking of lateral cells (compare Figure 4C,G with Figure 9C,E and Figure 11C,D). We suspected that the behavior of these cells might be controlled by the lateral Nodal signal which distinguishes them from their medial counterparts before the 64-cell stage (Hudson et al, 2007). To test this idea we performed time-lapse imaging on embryos electroporated with FoxD>Lefty, which inhibits Nodal signaling and causes lateral cells to express medial marker genes (Mita and Fujiwara, 2007).

Inhibition of Nodal signaling caused changes in both the timing of division and cell organization (Figure 14A-D). In contrast to control embryos (Figure 5), all row II cells entered the 10th generation within the same 15-minute window (Figure 14B,C) and entered the 11th generation prior to the mid-neurula stage. Lateral stacking was defective (Figures 14D, 18G,H) with A9.30, A9.29 and A9.32 derivatives failing to arrange themselves posterior to A9.16 on either side of the embryo. A9.14 and A9.16 derivatives made their usual oriented divisions, while A9.29 derived cells seemed to join the intercalary behavior of A9.15 and A9.13 derivatives, causing these movements to be disorganized.

The outcome of these altered behaviors is easily observed with phalloidin staining, which allowed us to quantify the phenotype using two diagnostic features: the presence of six columns of A-line derived cells at the mid-neurula stage and the addition of A9.29 derivatives to the floor plate, causing it to have twelve rather than eight cells (Figure 15A-D). The FoxD enhancer drives expression in A5.1, A5.2, and B5.1 blastomeres starting at the 16 cell stage (Mita and Fujiwara, 2007). To see if Nodal signaling is required beyond the early gastrula stage, we expressed Lefty using the later acting Etr enhancer. This had no effect on stacking, suggesting that Nodal is not required during these movements (Figure 16A-D).

To better understand the cellular behaviors underlying lateral stacking, we used the membrane targeted reporter YFP-CAAX to visualize the consequences of FoxD>Lefty electroporation in live embryos (Figure 15E). In contrast to control embryos, A9.29 failed to insert between A9.30 and A9.32. Furthermore, A9.30 remains adjacent to and divides simultaneously with A9.16, such that daughters of both cells end up side by side rather than aligned along the anterior-posterior axis. Together these changes are sufficient to explain the defects in lateral stacking already apparent at the early neurula stage (Figure 15E, 45').

To test whether Nodal signaling was sufficient to induce stacking behavior we ectopically

expressed Nodal in vegetal regions using a FoxD>Nodal fusion gene (see Mita and Fujiwara, 2007). Nuclei were visualized with a Snail>H2B:YFP reporter gene (Figures 14E,F; 19I,J). Nodal signaling induces Snail expression, and ectopic expression of Nodal results in ectopic activation of Snail in medial cells. Live imaging revealed that the timing of entry into the 10th generation was uncoordinated and overall development was delayed. Nevertheless, stacking of lateral cells appeared mostly normal. Furthermore, medial row I cells failed to properly intercalate while medial row II cells failed to enter the 11th generation by the mid-neurula stage.

The preceding results suggest that FGF controls intercalation of medial cells, whereas Nodal controls stacking of lateral cells. As a further test of this possibility we performed time-lapse imaging of embryos that lack both signals in the neural plate (ie. co-expression of FoxD>Lefty and FoxB>dnFGFR) (Figure 17A-C). In this experiment all cells of the A-line neural plate entered the 10th generation within the same 15-minute window and entered the 11th generation by the mid-neurula stage. All cell divisions are oriented along the AP axis, and there is an absence of the cellular rearrangements required for the formation of lateral stacks and midline intercalation (Figures 17C, 18K,L).

We next asked whether all A-line neural cells would participate in midline convergence if MAPK were activated in the absence of Nodal. To test this we performed live imaging on embryos lacking Nodal but misexpressing a constitutively activated form of MEK (co-expression of FoxD>Lefty and FoxB>caMEK transgenes) (Figure 17D-F). Under these conditions Mnx is expressed in all A-line neural cells suggesting a complete transformation to medial row I identity (Figure 16E). As expected for medial row I derivatives, all cells entered the 10th generation within the same 15 minute window, and did not enter the 11th generation by the mid-neurula stage. There is a dramatic midline convergence of both row I and row II derivatives, including separation of lateral sister cells which normally undergo stacking (Figure 17F, 18M,N). These results are consistent with the idea that FGF and Nodal independently specify intercalary and stacking behaviors of neural plate progenitor cells (see Discussion).

Discussion

We have presented evidence that Nodal and FGF signals deployed before completion of gastrulation coordinate the morphogenetic behaviors of A-line neural progenitor cells during neurulation (Figure 17G). FGF signaling is required for midline convergence of floor plate cells and is sufficient to induce intercalary behaviors in A-line cells not exposed to Nodal. Nodal signaling is required for proper stacking of lateral cells and inhibition of this signal causes these cells to adopt the behavior of their medial counterparts. In the absence of both FGF and Nodal signals neural tube progenitors adopt default behaviors that are typical of those seen for the progenitors of the sensory vesicle.

FGF/MAPK signaling and cellular morphogenesis

FGF signaling is critical for early vertebrate development and neural patterning (Böttcher and Niehrs, 2005) and is involved in numerous cell specification events during ascidian embryogenesis (e.g. Bertrand et al., 2003; Davidson et al., 2006; Wagner and Levine, 2012). Our study demonstrates that FGF signaling also controls the timing of cell

divisions and midline convergence of medial row I cells. Activation of canonical FGF/MAPK signaling or the downstream ETS-containing Elk transcriptional effector is sufficient to delay cell division and induce midline convergence, while inhibition of MAPK signaling after specification of medial row I fates does not alter the behavior of these cells. Together these results suggest that FGF/MAPK signaling during gastrulation is sufficient to simultaneously induce a floor plate identity and intercalary behaviors. Nevertheless, normal intercalation does rely on non-canonical FGF signaling after specification is complete. This situation is reminiscent of notochord morphogenesis, whereby canonical FGF/MAPK signaling at the 44-cell stage specifies notochord identity (Kim and Nishida, 2001; Nakatani and Nishida, 1997)but subsequent noncanonical FGF signaling is required for convergent extension (Shi et al., 2009). Future studies will identify the target genes responsible for the detailed cell behaviors underlying intercalation of the floor plate, including detachment of sister cell contacts. It will also be important to determine how this particular response to FGF signaling is achieved in contrast to the many other instances of MAPK-mediated FGF signaling during *Ciona* embryogenesis. FoxB is known to prevent notochord induction in response to FGF in the A-line neural lineage (Hashimoto et al., 2011) but it remains to be seen whether FoxB is sufficient to promote the development of floor plate cells in response to FGF.

Active junction contraction

There is evidence that diverse instances of convergent extension employ similar mechanisms of junction contraction (Shindo and Wallingford, 2014). We have provided evidence that such contraction might also underlie intercalation of the *Ciona* floor plate. However, there are also differences. For example, *Flamingo (Celsr*) and *Prickle* regulate intercalary behavior through the planar cell polarity pathway (Nishimura et al., 2012; Taniguchi and Nishida, 2004) but are absent in the floor plate. Curiously, these genes are expressed in the lateral neural plate, which undergoes stacking rather than convergence (Mita et al., 2010; Noda and Satoh, 2008).

We have also presented evidence that floor plate midline convergence is an active process, and not merely a passive consequence of delayed cell divisions. Nonetheless, a delay in division might contribute to the robustness of intercalation. Evidence that floor plate convergence is an active process agrees with previous work showing that the tail nerve chord undergoes extension even in the absence of notochord differentiation and extension (Di Gregorio et al., 2002).

Self-organization of the neural tube

Morphogenesis of the *Ciona* neural tube provides a simple and attractive model for understanding how complex structures arise from an initially undifferentiated group of cells. Indeed, we have shown that in the absence of FGF and Nodal signals all neural tube progenitors undergo the same program of oriented cell divisions as typically seen for the sensory vesicle. It is only through the influence of external signals that cells within this group adopt the unique behaviors necessary for proper neural tube morphogenesis. These signaling events are also used for cell specification, suggesting that transient cell states influence morphogenetic behaviors of cells enroute to their ultimate identities.

Intriguingly, we find that the signals establishing these states are deployed prior to the completion of gastrulation, while the behaviors they confer are not fully realized until the onset of neurulation. Understanding how these states arise and in turn influence cellular morphogenesis promises to be a continuing challenge in the quest to discover how anatomy is encoded in the genome.

Figure 9

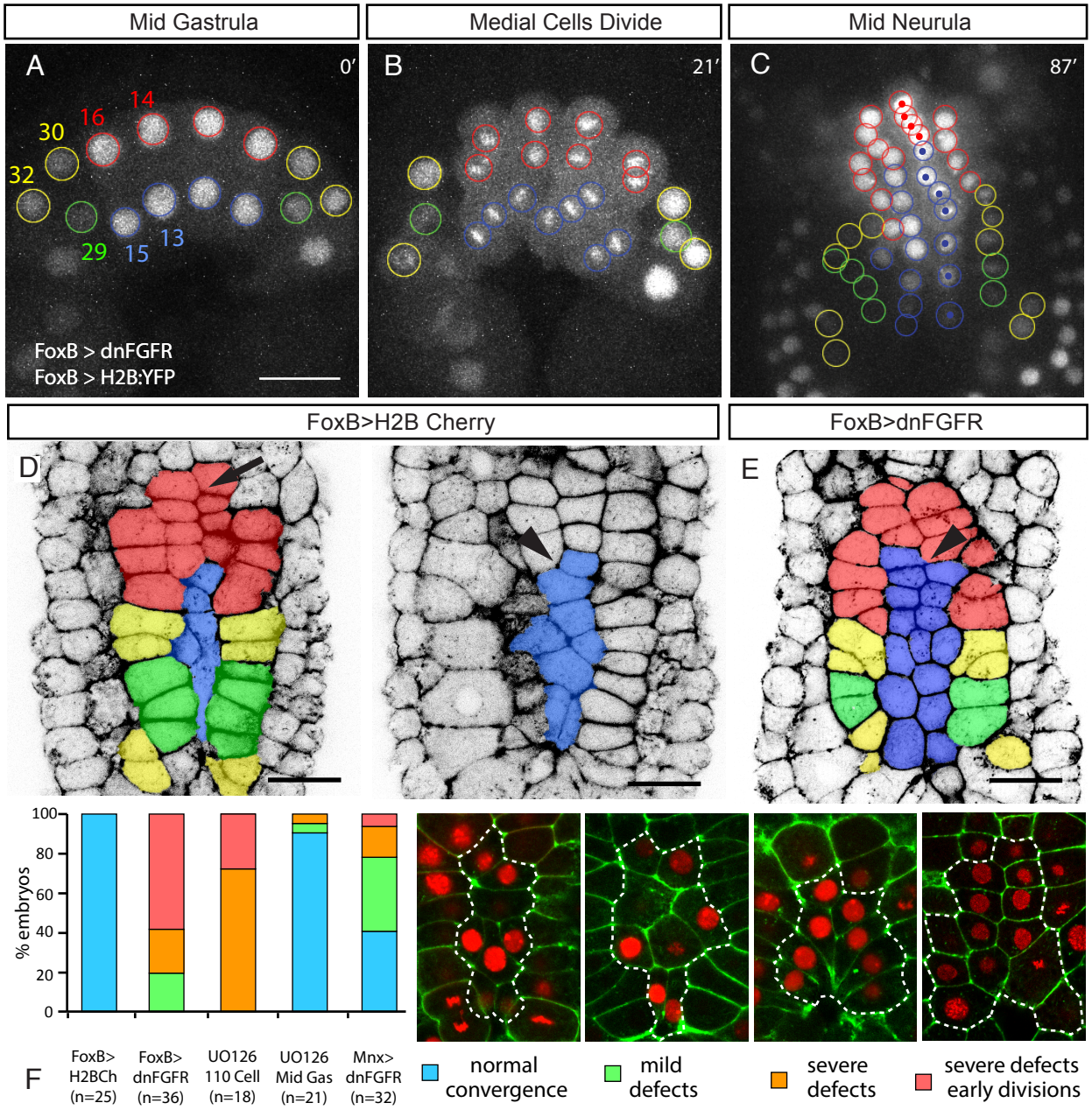
Mid Gastrula
Medial Cells Divide
Mid Neurula
A
0′
B
21′
C
87′
14
16
30
32
29
15
13
FoxB > dnFGFR
FoxB > H2B:YFP
FoxB>H2B Cherry
FoxB>dnFGFR
D
E
% embryos
100
80
60
40
20
0
F
FoxB> H2BCh (n=25)
FoxB> dnFGFR (n=36)
UO126 110 Cell (n=18)
UO126 Mid Gas (n=21)
Mnx> dnFGFR (n=32)
normal convergence
mild defects
severe defects
severe defects early divisions

Figure 9: FGF/MAPK is required for midline convergence of floor plate cells. (A-C) Time lapse confocal microscopy of embryo co-electroporated with FoxB>dnFGFR and FoxB>H2B:YFP. Cell lineages are color coded as in Fig. 1 and right side nuclei at the midline are indicated with a spot. (B) Derivatives of A9.14,16,13 and 15 divide simultaneously (n=3/3). (C) At mid-neurula stage most A9.13 and A9.15 derived cells have divided twice and failed to cross the midline (n=3/3). (D, E) False colored phalloidin stained mid-neurula embryos electroporated with FoxB>H2B:Cherry alone (D) and FoxB>dnFGFR together with FoxB>H2B:Cherry (E). In control embryos A9.14 derivatives are confined to either side of the midline (arrow) while A9.13 and A9.15 derivatives converge, interrupting the membrane spanning the midline (arrowhead). In embryos electroporated with FoxB>dnFGFR this midline span continues between left and right A9.13 and A9.15 derived cells (arrowhead). (F) Quantification of phenotypes for the indicated treatment. When convergence is normal, multiple floor plate cells are in contact with lateral cells from the left and right sides. Slight defects are defined by some rearrangement of floor plate cells with one or fewer cells spanning left and right lateral cells. Severe defects occur when floor plate cells are entirely confined to the side of the embryo where they originated; early divisions occur when one or more of these cells has entered the 11^{th} generation by the mid-neurula stage. FoxB>H2B:Cherry total consists of 12 embryos co-electroporated with FoxB>LacZ and 13 embryos treated with DMSO at the 110 cell stage. Totals are from two independent experiments. All scale bars are 25μm.

Figure 10

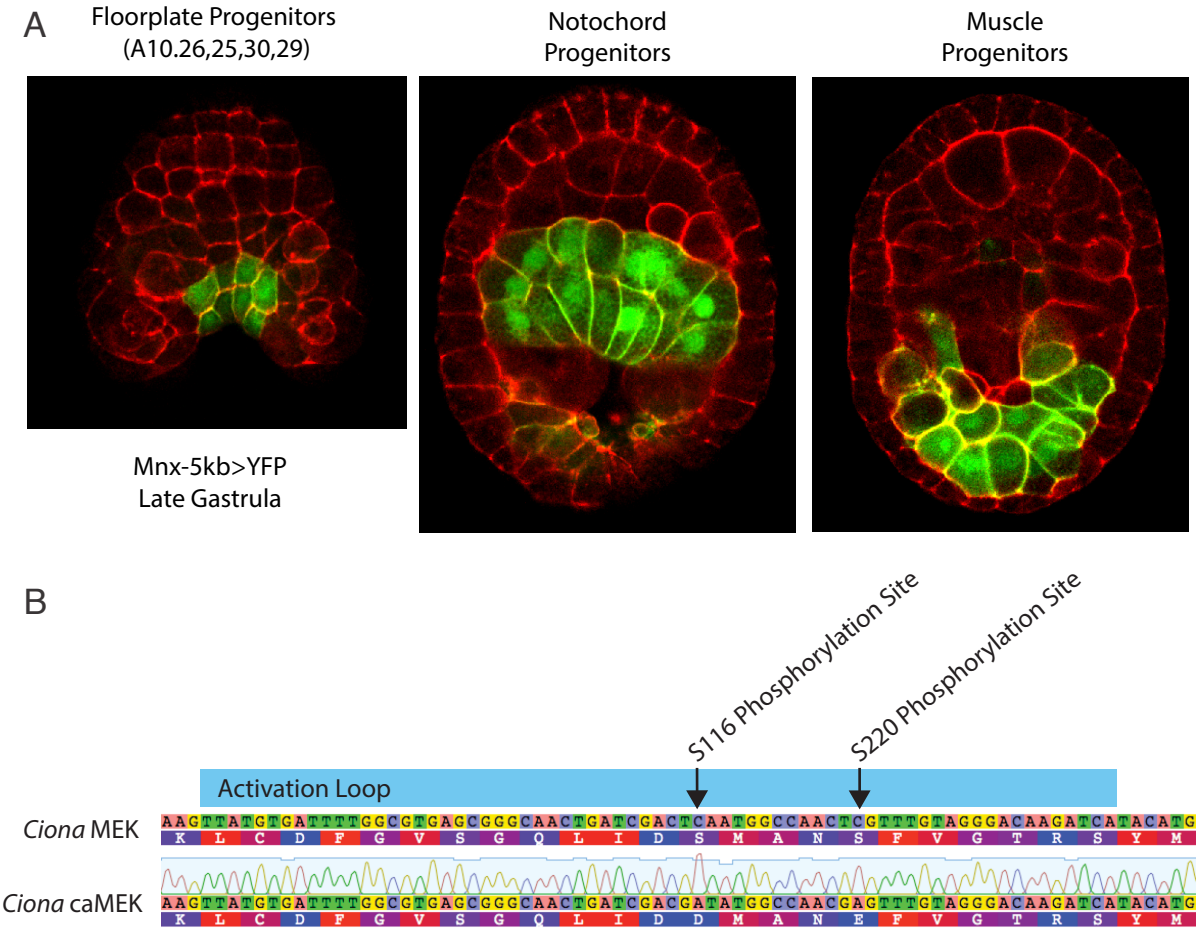

Mnx enhancer and caMEK construction. (A) Expression of the Mnx -5kb enhancer at the late gastrula stage. Mnx>YFP in green and phalloidin staining in red. Each image is a slice from the same embryo through the indicated tissue. (B) Sequencing results of caMEK gene confirming modified phosphorylation sites in the MEK activation loop.

Figure 11

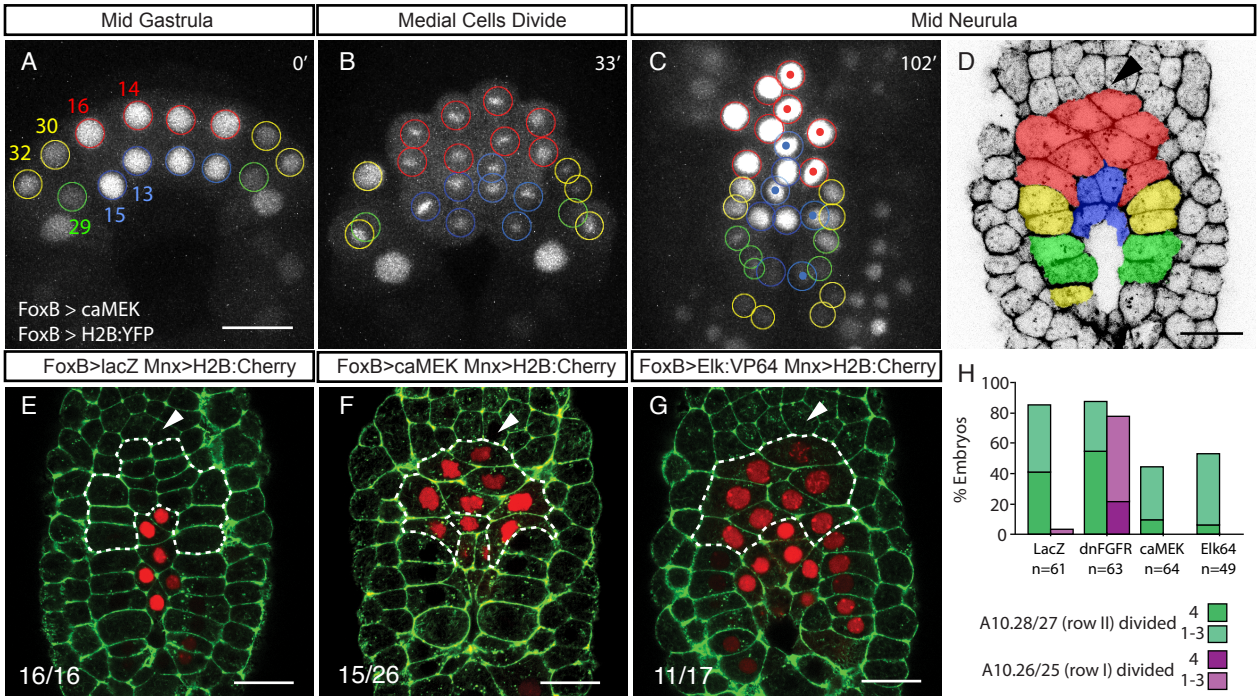

FGF/MAPK acting through Ets/Elk family transcription factors delays cell division and promotes midline convergence of medial cells. (A-C) Time lapse confocal microscopy of embryo co-electroporated with FoxB>-caMEK and FoxB>H2B:YFP (B) Derivatives of A9.14,16,13 and 15 divide simultaneously (n=6/7). (C) At mid-neurula stage A9.14 and A9.16 derivatives (red) have failed to enter the 11th generation and have converged towards the midline (n=5/7). (D) False colored phalloidin stained mid-neurula embryo electroporated with FoxB>-caMEK and FoxB>H2B:Cherry. Arrowhead indicates where midline membrane is interrupted by A9.14 derivative. (E-G) Mid-neurula stage embryos electroporated with indicated transgenes and stained with phalloidin. Dotted line outlines A9.14/A9.16 derivatives. (E) Mnx reporter is limited to A9.13 and A9.15 derived floor plate cells. (F,G) Ectopic Mnx expression is seen in A9.14 and A9.16 derivatives. In both cases these cells also interrupt the midline membrane (arrows). Floor plate cells are deeper within embryo. Indicated n is the number of embryos which exhibit ectopic Mnx reporter expression in combination with delayed division and midline convergence of A9.14/A9.16 derivatives. Totals are from two independent experiments. (H) Quantification of A9.14 and A9.13 derivatives which have entered the 11th generation by the mid-neurula stage. Embryos were electroporated with FoxB driving the indicated gene and FoxB>H2B:Cherry to aid quantification. Totals are from two independent experiments. All scale bars are 25µm.

Figure 12

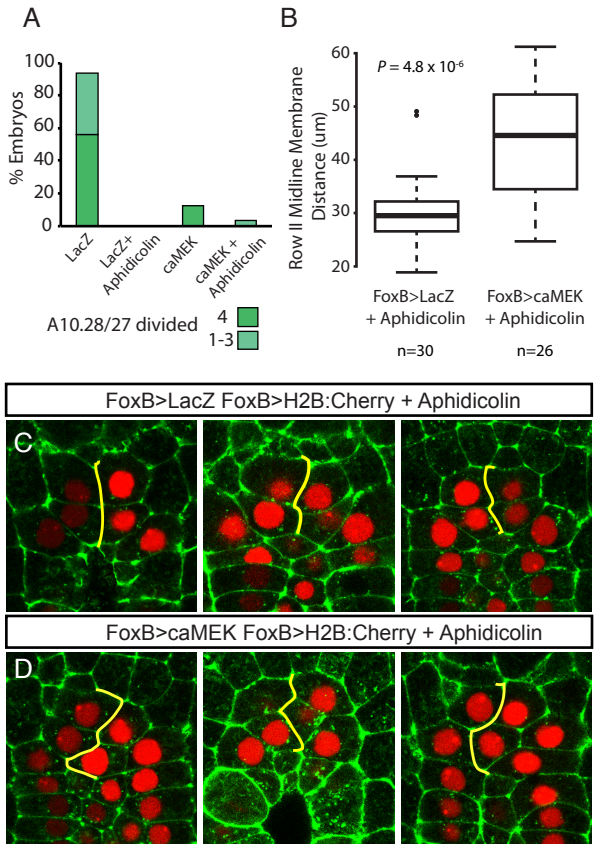

Cell Cycle delay is not sufficient for full midline convergence. (A) Quantification of A9.14 derivatives which have entered the 11th generation by the mid-neurula stage. Embryos were electroporated with FoxB driving the indicated gene and FoxB>H2B:Cherry to aid quantification. Aphidicolin treatment was carried out at the late gastrula stage. Number of embryos counted totaled from 4 independent experiments: LacZ: 16, LacZ + Aphidicolin: 30, caMEK: 16, caMEK + Aphidicolin: 28. (B) Box plot summary of midline membrane span length between A9.14 derivatives at mid-neurula stage. Measurements were performed manually with ImageJ software. Statistical significance calculated with Wilcoxon two-sample test. (C,D) Examples of membrane span traces used to create data in (B). Embryos are electroporated with the indicated transgenes and treated with aphidicolin.

Figure 13

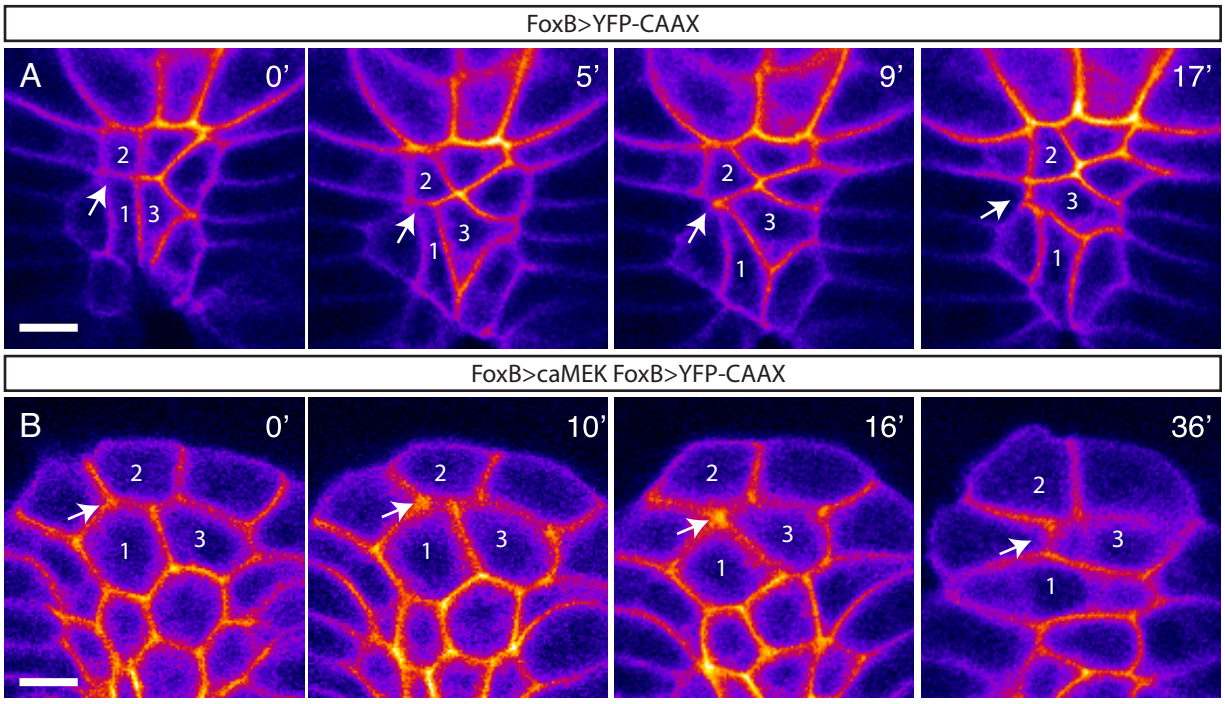

Junction rearrangement during midline convergence: Stills from time lapse live imaging of embryos electroporated with the indicated transgenes. Numbers mark the same cell from one frame to the next with cell 3 inserting between cells 1 and 2 in both cases. Arrow indicates rearrgangment of junction configuration between cells 1 and 2. Pseudo-color look up table was chosen to increase membrane visibility. (A) Intercalation of medial row I cells. 1: A10.25 (left), 2: A10.26 (left), 3: A10.25 (right). (B) Intercalation of medial row II cells. 1: A10.27 (left), 2: A10.28 (left), 3: A10.27 (right). Scale bars are 10µm.

Figure 14

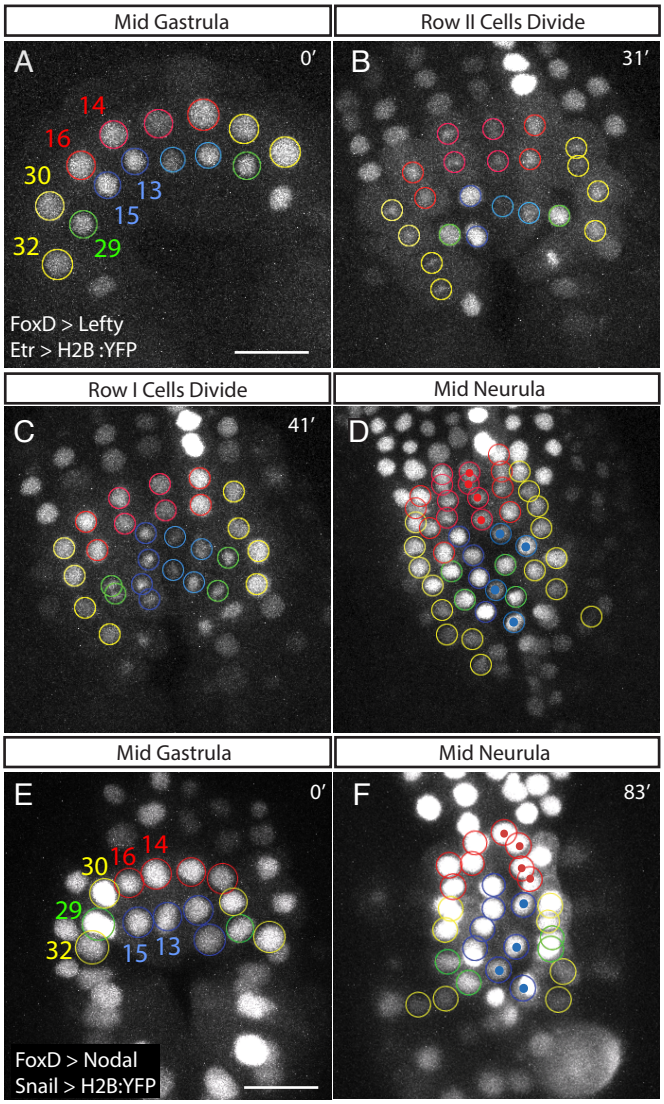

Nodal influences timing of division and is required for proper lateral stacking during neurulation. Time lapse stills visualizing H2B:YFP. Cell lineages are color coded as in Figure 1 and right side nuclei at the midline are indicated with a spot. (A-D) Embryo electroporated with FoxD>Lefty and Etr> H2B:YFP. (B, C) All cells belonging to row II divide simultaneously followed by all cells in row I (n=5/5). (D) Lateral stacking of A9.32,30,29 and 16 is disrupted and lateral row II cells have prematurely reached the 11th generation (n=6/6). (E,F) Embryo electroporated with FoxD>Nodal and Snail>H2B:YFP. (F) A9.14/16 cells (red) have failed to enter 11th generation by mid-neurula stage and lateral stacking of A9.32,30,29 and 16 is normal (n=3/3). Scale bars are 25µm.

Figure 15

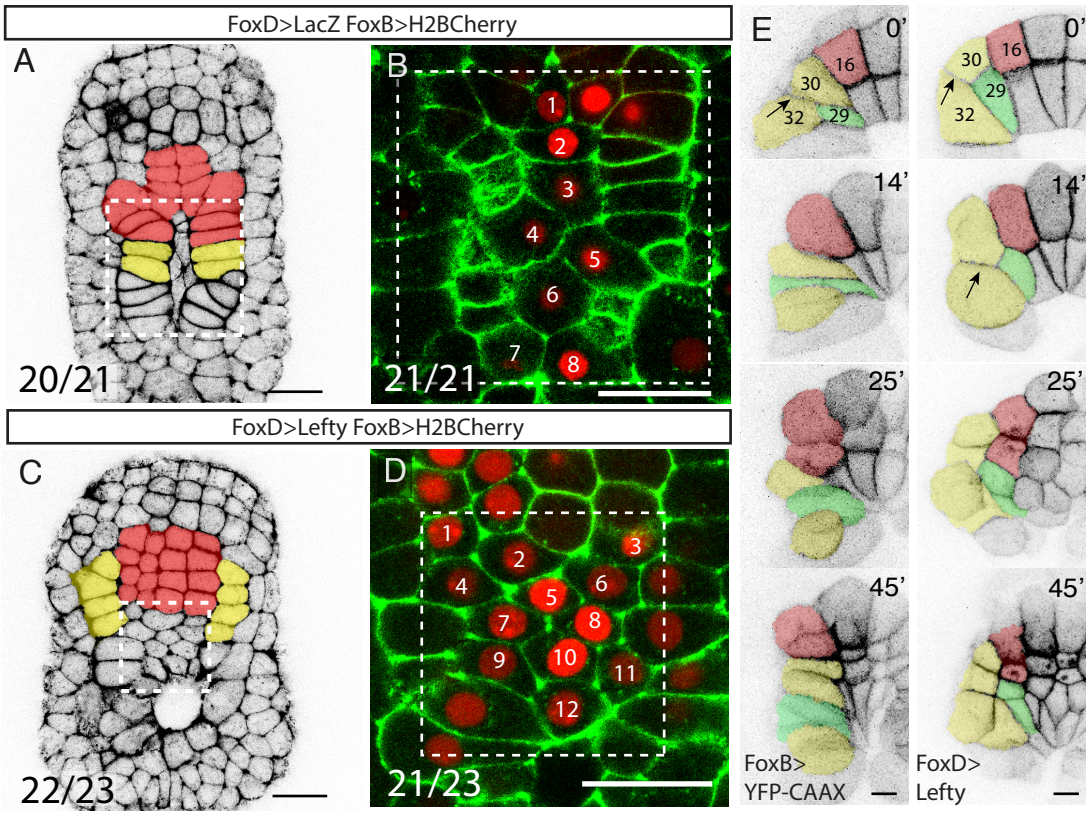

Stacking defects caused by Nodal inhibition: (A-D) Embryos electroporated with the indicated transgenes and fixed at the mid-neurula stage. (A,C) False colored, phalloidin stained embryos with n value indicating number of embryos exhibiting 4 columns of A-line cells (A) or 6 columns (C). (B,D) Counting of floor plate cells. Dashed box indicates same region of embryo as (A,C). N value indicates number of embryos with 8 floor plate cells (B) or 12 floor plate cells (C). Totals are from two independent experiments. Scale bars are 25µm. (E) False colored stills from time lapse live imaging of embryos electroporated with FoxB>YFP-CAAX alone (left) and in combination with FoxD>Lefty (right). Arrows indicate junction between A9.30 and A9.32. Scale bars are 10µm.

Figure 16

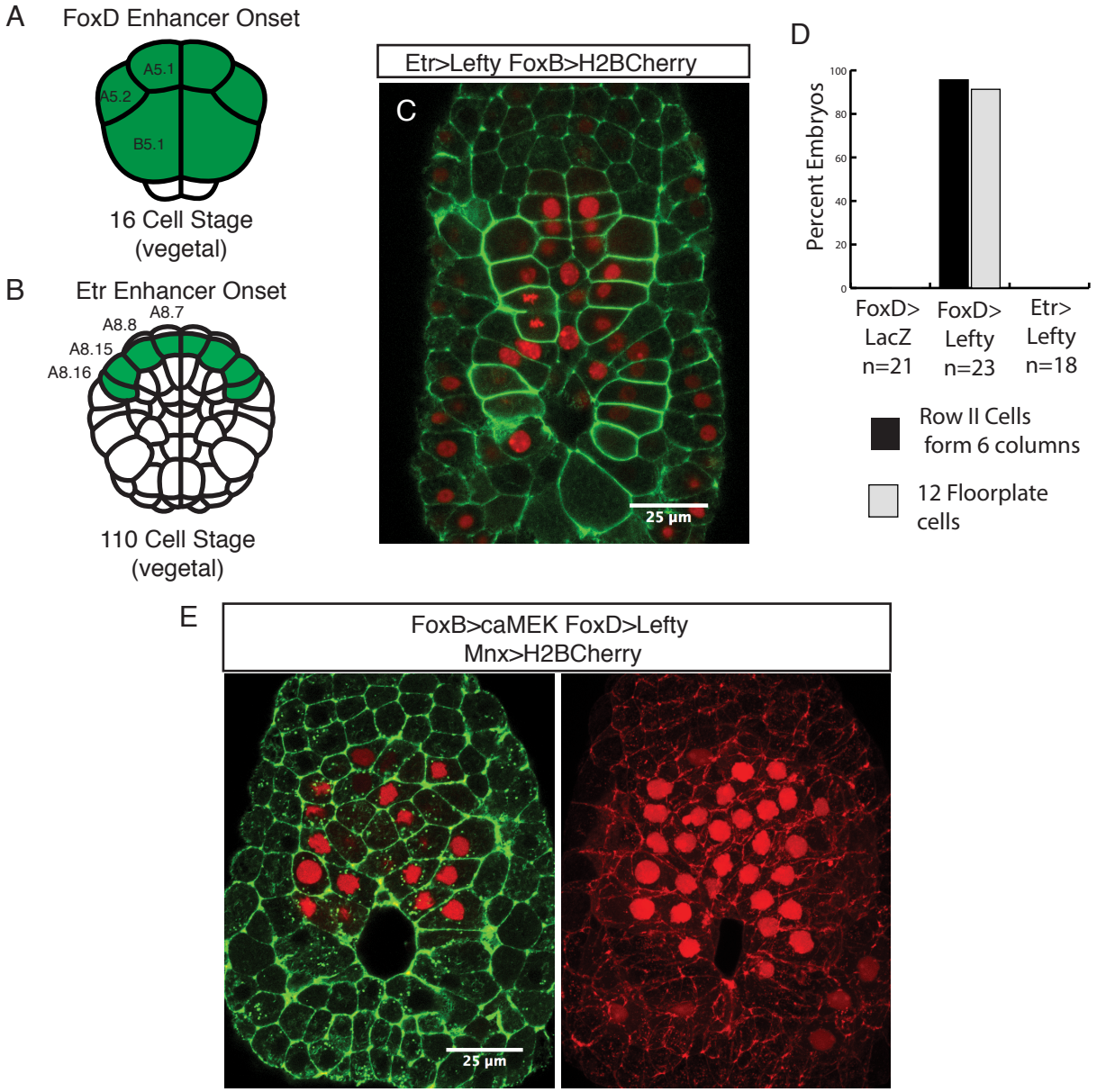

Timing and consequences of Nodal inhibition. (A) Cartoon showing onset of FoxD enhancer activity at the 16-cell stage. A5.1, A5.2 and B5.1 blastomeres which initially express FoxD are colored green. The enhancer drives later expression in the daughters of these cells at the 32-cell stage and broadly on the vegetal side of the embryo during gastrulation (Mita and Fujiwara, 2007). (B) Cartoon showing onset of Etr enhancer activity at the 110-cell stage. A8.7, A8.8, A8.15 and A8.16 blastomeres which initially express Etr are colored green. The enhancer drives later expression in all A- and a-line neural cells (Veeman et a. 2010). (C) Representative mid-gastrula stage embryo electroporated with Etr>Lefty and FoxB>H2B:Cherry. (D) Quantification of lateral stacking defect phenotypes at the mid-neurula stage (see Fig. 9). (E) Confocal image of phalloidin stained embryo electroporated with FoxD>Lefty, FoxB>caMEK and Mnx>H2B:Cherry. Single slice with phalloidin staining in green (Left) and maximum projection H2B:Cherry expressing nuclei (right). 5 of 7 embryos had ectopic reporter expression in both medial row II and lateral cells of both rows.

Figure 17: Oriented divisions are a morphogenetic ground state for the A-line neural lineage which is modified by FGF/MAPK and Nodal signaling. (A-C, D-F) Stills from time lapse live imaging of embryos electroporated with the indicated transgenes and FoxB>H2B:YFP reporter. Cell lineages are color coded as in figure 1B. Where cells from the left and right sides of the embryo mix right side cells are indicated by a dot within the nucleus. (B, E) Late-gastrula stage embryos exhibit similar phenotypes in the presence and absence of FGF/MAPK signaling. (C) Combined Nodal and FGF inhibition causes all A-line neural cells to enter the 10^{th} generation within same 15 minute window (n=5/6) and enter 11^{th} generation by mid-neurula stage without midline convergence or lateral stacking (n=6/6). (F) When MAPK signaling is activated in the absence of Nodal signaling all cells enter the 10^{th} generation within same 15 minute window (n=3/6) and no cells enter the 11^{th} generation by the mid-gastrula stage (n=4/7). Ectopic intercalations are present among both medial and lateral cells (n=4/7). (G) Visual summary of findings. Top row: At the late gastrula stage cells have entered the 10^{th} generation via an anterior-posterior oriented division and are positioned next to their sister cells. Midline is indicated by a dotted line. Bottom row: In the absence of earlier Nodal and FGF signals, cells divide again in an anterior-posterior orientation maintaining their position relative to the midline. When MAPK is activated in the absence of Nodal, cells delay their division and converge at the midline becoming separate from their sister cells. If cells receive have received a Nodal signal entry into the 11^{th} generation is delayed and cells form lateral stacks without losing contact with their 10^{th} generation sisters. Opposing arrowheads between cells indicate the most recent cell division.

Figure 17

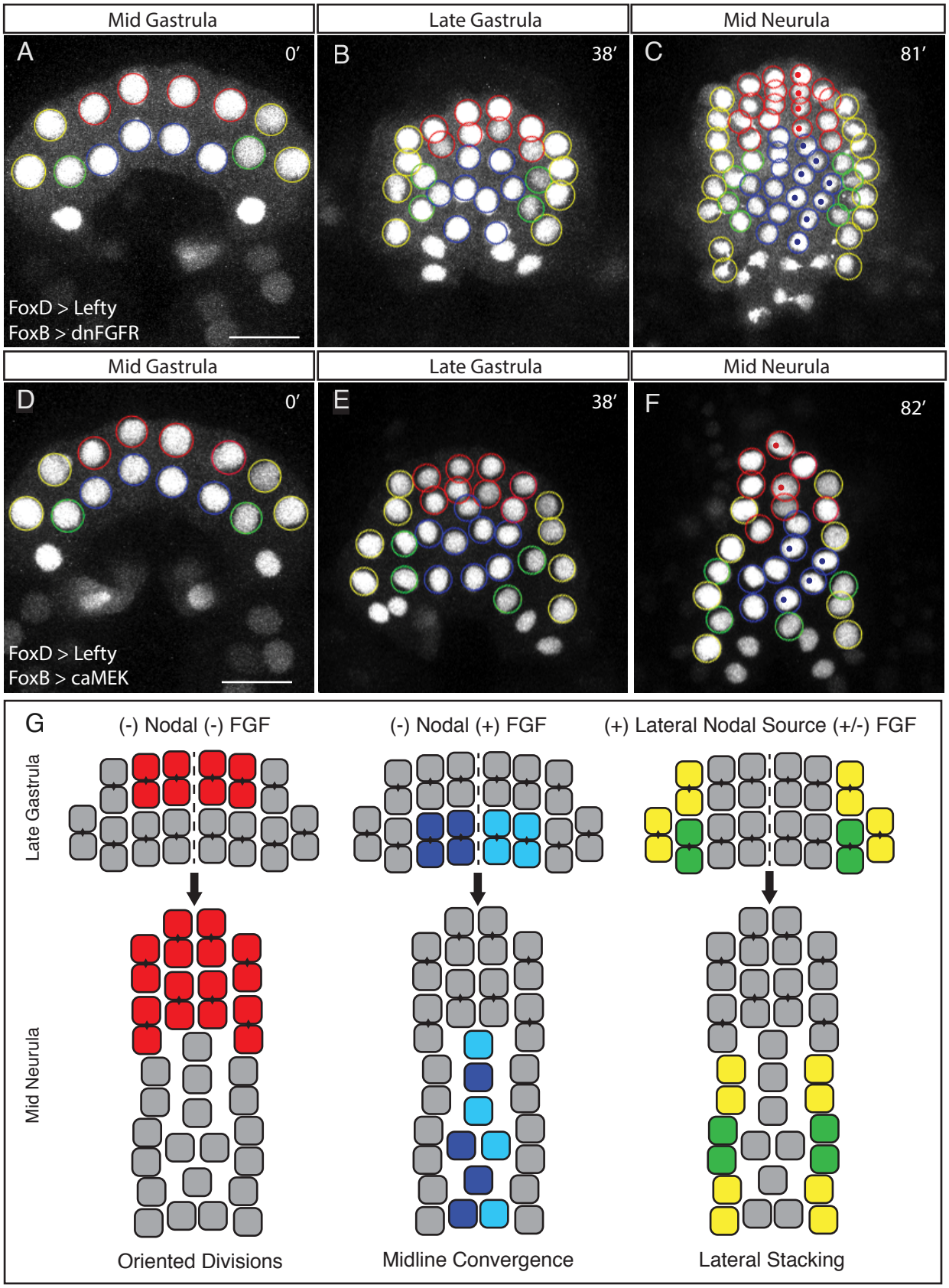
Mid Gastrula
Late Gastrula
Mid Neurula
A
0′
B
38′
C
81′
FoxD > Lefty
FoxB > dnFGFR
Mid Gastrula
Late Gastrula
Mid Neurula
D
0′
E
38′
F
82′
FoxD > Lefty
FoxB > caMEK
G
(-) Nodal (-) FGF
(-) Nodal (+) FGF
(+) Lateral Nodal Source (+/-) FGF
Late Gastrula
Mid Neurula
Oriented Divisions
Midline Convergence
Lateral Stacking

Figure 18: Live imaging replicate outcomes at the mid-neurula stage. (A-N) Maximum projection stills from time-lapse experiments with circles showing the locations of A-line neural cells at the mid-neurula stage. Embryos were electroporated with the indicated transgenes. Colors follow lineage scheme from Fig. 1 with, dots indicating right side cells at the midline. All scale bars are 25μm.

Figure 18

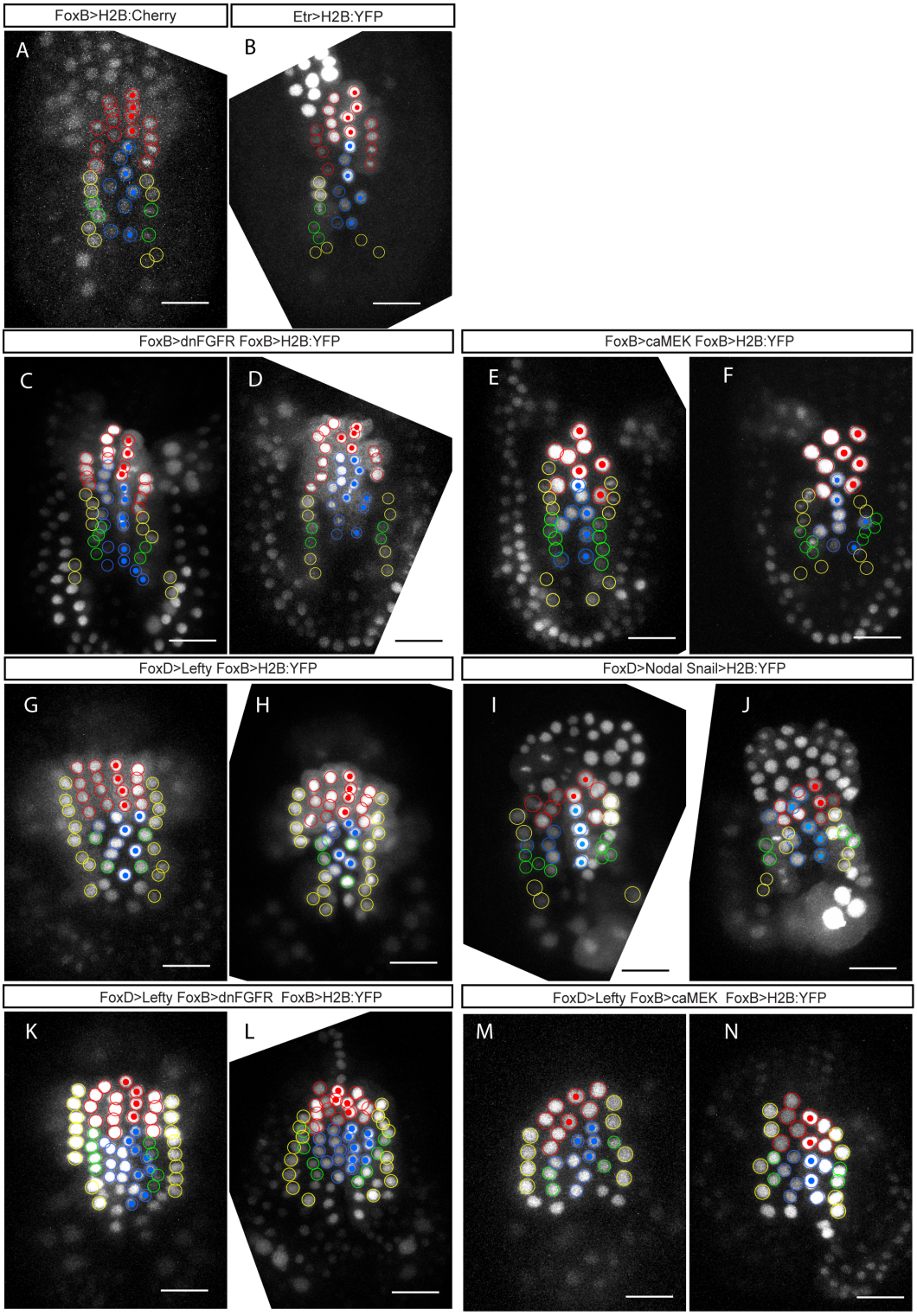
FoxB>H2B:Cherry
Etr>H2B:YFP
A
B
FoxB>dnFGFR FoxB>H2B:YFP
FoxB>caMEK FoxB>H2B:YFP
C
D
E
F
FoxD>Lefty FoxB>H2B:YFP
FoxD>Nodal Snail>H2B:YFP
G
H
I
J
FoxD>Lefty FoxB>dnFGFR FoxB>H2B:YFP
FoxD>Lefty FoxB>caMEK FoxB>H2B:YFP
K
L
M
N

Table 1

Perturbation	Plasmids	Figure Locations	A9.14 cells reach 11th gen by mid-neurula stage, no intercalation	Eight 11th generation A9.29 cells at late neurula stage	A10.64 migrates anteriorly		Additional Comments
None	FoxB>H2B:YFP, FM 464 Staining		yes	yes	-		Only Left A9.30/A9.29 derivatives are labled. Order of floorplate intercalation from anterior to posterior is right A9.26, left A9.26, right A9.25.
	Etr>YFP-CAAX		yes	-	-		Difficult to track cells but can see floorplate intercalation. Order of floorplate intercalation from anterior to posterior is right A9.26, left A9.26, right A9.25.
	Etr>H2B:YFP	Fig. S5B	yes	yes	-		Only left side has reporter. Order of floorplate intercalation from anterior to posterior is right A9.26, left A9.26, right A9.25.
	FoxB>H2B:YFP FoxB>LacZ	Fig. 2,3 Movie 8	yes	yes	yes		Left side epidermal nuclei have some DNA bridging when dividing but all A-line neural cells look good. Order of floorplate intercalation from anterior to posterior is left A9.26, right A9.26, left A9.25.
	FoxB>YFP-CAAX	Fig. 7A Movie 4	yes	yes	-		Order of floorplate intercalation from anterior to posterior is right A9.26, left A9.26, right A9.25.
	FoxB> H2B:Cherry	Fig. S5A	yes	yes	yes		Can see membrane contraction in floorplate cells. Order of floorplate intercalation is right A9.26, left A9.26, right A9.30, right A9.25.
	FoxB>YFP-CAAX	Fig. 9E	yes	yes	yes		Order of floorplate intercalation from anterior to posterior is left A9.26, right A9.26, left A9.25.
Perturbation	**Plasmids**	**Figure Locations**	**Medial cells divide together**	**A9.13 and A9.15 enter 11th generation early and fail to intercalate**			**Additional Comments**
Fgf inhibition	FoxB>dnFGFR, FoxB>H2B:YFP	Fig. S5D	yes	yes			Slight DNA bridging
	FoxB>dnFGFR, FoxB>H2B:YFP	Fig. S5C	yes	yes			DNA bridging on right side
	FoxB>dnFGFR, FoxB>H2B:YFP	Fig. 4A-C Movie 2	yes	yes			Slight DNA bridging

Perturbation	Plasmids	Figure Locations	Medial cells divide together	Medial Row II division delayed	Midline convergence of A9.14		Additional Comments
MapK activation	FoxB>caMEK, FoxB>H2B:YFP		yes	yes	yes (similar to Fig. S5F)		
	FoxB>caMEK, FoxB>H2B:YFP	Fig. S5F	yes	yes	yes (see Fig. S5F)		
	FoxB>caMEK, FoxB>H2B:YFP	Fig. S5E	yes	yes	yes		
	FoxB>caMEK, FoxB>YFP:CAAX	Fig. 7B Movie 5	yes	yes	yes, junction contraction visible		
	FoxB>caMEK, FoxB>H2B:YFP		yes	yes	no		
	FoxB>caMEK, FoxB>H2B:YFP	Fig. 5A-C Movie 3	yes	yes	yes		
	FoxB>caMEK, FoxB>H2B:YFP		no	no	no		
Perturbation	**Plasmids**	**Figure Locations**	**Row II cells divide simultaneously**	**Row I cells divide simultaneously**	**A9.30 derivatives fail to move behind A9.16**	**A9.13 derivatives fail to stack**	**Additional Comments**
Nodal Inhibition	FoxD>Lefty, Etr>H2B:YFP	Fig. 8A-D Movie 6	yes	yes	yes	yes	
	FoxD>Lefty, FoxB>H2B:YFP	Fig. S5H	yes	yes	yes	yes	Some DNA bridging
	FoxD>Lefty, FoxB>H2B:YFP	Fig. S5G	-	-	yes	yes	Starts at late gastrula stage
	FoxD>Lefty, FoxB>YFP-CAAX	Fig. 9E, Movie 8	yes	yes	yes	yes	
	FoxD>Lefty, FoxB>YFP-CAAX		yes	yes	yes	yes	
	FoxD>Lefty, FoxB>YFP-CAAX		yes	yes	yes	yes	
Perturbation	**Plasmids**	**Figure Locations**	**Lateral Stacking OK**	**A9.14 delayed divison**	**Floor plate intercalation abnormal**		**Additional Comments**
Nodal Addition	FoxD>Nodal, Snail>H2B:YFP	Fig. S5I	yes	yes	yes		
	FoxD>Nodal, Snail>H2B:YFP	Fig. 8E,F	yes	yes	yes		
	FoxD>Nodal, Snail>H2B:YFP	Fig. S5J	yes	yes	yes		

Perturbation	Plasmids	Figure Locations	Simultaenous divisions into 10th generation for all cells	All cells enter 11th geneartion at mid-neurula stage without intercalation or stacking			Additional Comments
Nodal Inhibition + FGF Inhibition	FoxB>H2B:YFP FoxD>Lefty FoxB>dnFGFR		yes	yes			DNA bridging when cells divide
	FoxB>H2B:YFP FoxD>Lefty FoxB>dnFGFR	Fig. 10A-C, Movie 9	yes	yes			Slight DNA bridging when cells divide
	FoxB>H2B:YFP FoxD>Lefty FoxB>dnFGFR	Fig. S5K	yes	yes			
	FoxB>H2B:YFP FoxD>Lefty FoxB>dnFGFR	Fig. S5L	no	yes			2 A -line cells have delayed division but otherwise shows phenotype
	FoxB>H2B:YFP FoxD>Lefty FoxB>dnFGFR		yes	yes			slight DNA bridging when dividing
	FoxB>H2B:YFP FoxD>Lefty FoxB>dnFGFR		yes	yes			slight DNA bridging when dividing
Perturbation	**Plasmids**	**Figure Locations**	**Simultaneous divisions into 10th generation for all cells**	**11th generation cells at mid-neurula stage**	**Ectopic intercalations**		**Additional Comments**
Nodal Inhibition + MAPK Activation	FoxD>Lefty, FoxB>caMEK, FoxB>H2B:YFP	Fig. 10D-F, Movie 10	yes	no	yes, 5		
	FoxD>Lefty, FoxB>caMEK, FoxB>H2B:YFP	Fig. S5M	yes	no	yes, 3		
	FoxD>Lefty, FoxB>caMEK, FoxB>H2B:YFP	Fig. S5N	yes	yes	yes, 2		
	FoxD>Lefty, FoxB>caMEK, FoxB>H2B:YFP		no	yes	no		Left side has FoxD>lefty phenotype, right side has FoxB>caMEK + FoxD>Lefty
	FoxD>Lefty, FoxB>caMEK, FoxB>H2B:YFP		-	no	yes, 2		starts at late gastrula stage
	FoxD>Lefty, FoxB>caMEK, FoxB>H2B:YFP		no	yes	no		Only 2 medial colums have FoxB>caMEK phenotype , other are FoxD>Lefty only
	FoxD>Lefty, FoxB>caMEK, FoxB>H2B:YFP		no	no	yes, 2		

Chapter 5: Future Perspectives

Over the course of my dissertation work and thinking about the A-line neural lineage, I have made a few observations, based in large part on existing literature, which I have not been able to pursue experimentally. Specifically, these observations concern floor plate induction, the evolutionary relationships between the A-line derived portions of the sensory vesicle and the vertebrate brain, and the cellular effector genes which link specification and morphogenesis. I have included these observations in this chapter in the hope that they will be of use to future researchers interested in these cells.

Floor plate induction

It is clear that FGF signaling acting through the MAPK pathway and Ets family transcription factors is critical for the specification and intercalation behavior of floor plate cells. Even so, there are a number of interesting questions surrounding this induction which remain to be fully elucidated.

The first question is that of the source of the FGF signal. Based on in-situ hybridizations, a good candidate is *FGF9/16/20*, which is expressed in A-line neural precursors at the early gastrula stage when the signal specifying row I cells is transduced (Hudson et al., 2007; Imai et al., 2006). If this is indeed the source of subsequent MAPK activation in row I, it means that the signal is acting in an autocrine capacity in the A-line neural lineage. This suggests that rather than a posteriorly localized source of FGF, it could be an anterior inhibitor of FGF signaling which is responsible for the differential MAPK activity in 9th generation A-line neural cells. Based on the similarities to notochord induction (Picco et al., 2007), an ephrin signal emanating from the a-lineage would seem to be a likely candidate for this role.

In an attempt to test this idea, we electroporated the FoxB enhancer driving a dominant negative form of the Eph3 receptor. This transgene is able to transform A-line neural cells into notochord (Picco et al., 2007), and also disrupt fates relying on downregulation of MAPK within the trunk ganglion (Stolfi et al., 2011). Despite this, electroporation of FoxB>dnEph3 had no apparent effect on A-line neural fates. Looking for alternative possibilities, I noticed that among the *Ciona* Eph genes there is a receptor closely related to *Ci-Eph3*, *Ci-Eph5*, for which there is no published in-situ (Satou et al., 2003). Interestingly, the Ephrin ligand responsible for inhibition of notochord fate at the 32-cells stage (*Ci-Ephrin A-D*) also has a closely related homologue, *Ci-Ephrin A-C*, which is expressed in the a-lineage at 64 through 110-cell stages, precisely the time when required for down regulation of MAPK in the A-line neural lineage (Imai et al., 2004; Satou et al., 2003).

Attempts to test whether *Ci-Eph5* is responsible for MAPK down regulation in row II cells were hampered by the apparent toxicity of this gene to *E. coli*. Possible ways to overcome this difficulty include using a low-copy number plasmid backbone and *E. coli* strains with tighter control of plasmid expression or resistance to transmembrane protein toxicity (Miroux and Walker, 1996). If *Ci-EphrinA-C* and *Ci-Eph5* do turn out to be responsible for MAPK downregulation in the A-lineage, it would provide a nice example

responsible for MAPK downregulation in the A-lineage, it would provide a nice example of sub-functionalization and a co-evolution of ligand receptor pair, as well as further evidence for an evolutionary link between the notochord and floor plate. This link evolutionary link is suggested by shared locations of embryonic origin (Peyrot et al., 2011) and patterns of gene expression (Dal-Pra et al., 2011). It would also be interesting to see whether the Eph-ephrin duplication is present in all ascidians, or is unique to a particular clade.

As noted earlier, another key question is how floor plate induction is achieved in contrast to the many other FGF dependent fates during ascidian embryogenesis. On possibility is that the presence of FoxB is important for the correct interpretation of MAPK activation. To test this, one could express FoxB in the A-lineage from the 32-cell stage using the Zicl or FoxD enhancer and then see whether A-line cells adopt a floor plate rather than notochord fate in response. A positive outcome for this experiment should result in *Mnx* activation in the absence of *Brachyury* and the expression of *Unc4*, a floor plate specific marker (Figure 19), during tailbud stages.

Evolutionary links of A9.14 derived photoreceptor cells

It is now clear that the photoreceptors of the ocellus are derived from A9.14 rather than the a-lineage (Oonuma et al., 2016). As a result, we can begin to investigate the evolutionary links between these cells and corresponding portions of the vertebrate brain. It has been suggested that ascidian photoreceptor cells might be related to pineal organ photo receptors (Kusakabe and Tsuda, 2007), retinal cells of vertebrates (Oonuma et al., 2016), or perhaps a structure ancestral to both the retina and hypothalamus (Razy-Krajka et al., 2012). Each of these structures is derived from the diencephalon, so to address this question it is first important to determine whether or not the A9.14 lineage has evolutionary links to this part of the brain. Establishing homology between distantly related structures is a difficult task, but a relatively strong case can be made if the structures can be shown to have three key characteristics: 1) shared cell types or cell behaviors 2) shared territories of embryonic origin 3) conserved portions of a gene regulatory network. Ascidian photoreceptors have clear physiological links to those in vertebrates (Kusakabe and Tsuda, 2007), so to figure out if there are more direct links to any particular group of vertebrate photoreceptors requires additional data on shared embryonic territories and gene networks.

Despite strong evidence for homology, relating the organization of the ascidian nervous system to that of vertebrates has been complicated by gene loss and divergent expression patterns of key markers (Ikuta and Saiga, 2007). As a result, a few different models have been proposed (Dufour et al., 2006; Ikuta and Saiga, 2007; Sasakura et al., 2003; Wada et al., 1998). Nevertheless, it has been suggested that major portions of the sensory vesicle have evolutionary links to the diencephalon (Moret et al., 2005). Indeed, since most evidence suggests that the telencephalon is a vertebrate innovation (e.g. Oda and Saiga, 2001), it seems reasonable to suppose that much of the sensory vesicle could be related to the diencephalon. In the case of the A9.14 lineage it is counterintuitive that these posteriorly derived cells could be linked to a forebrain structure, yet there is some evidence in favor of this idea. Specifically, these cells are within a domain of overlapping

Otx and *FoxB* expression and seem to expresses *Pax6* but not *Engrailed* (which appears to be in A9.16 derivatives) at the early-tailbud stage (Hudson et al., 2003; Ikuta and Saiga, 2007; Imai et al., 2004). Overlapping expression of *Otx* and *FoxB* suggests that these cells could be related to either the vertebrate forebrain or midbrain. In vertebrates *Pax6* marks the diencephalic side of the diencephalon-midbrain boundary, while *Engrailed* marks the more posterior midbrain (Scholpp et al., 2003). Loss of Pax6 leads to an anterior expansion of midbrain markers while ectopic expression seems to expand the diencephalon at the expense of the midbrain. Conversely, loss of Engrailed leads to an expansion of *Pax6*, while ectopic Engrailed expands the midbrain at the expense of the diencephalon (Scholpp et al., 2003). Although the expression of these genes (Ikuta and Saiga, 2007) and some of the interactions between them have been tested in *Ciona* (Imai et al., 2009), a more detailed analysis is warranted to see if the interactions observed in vertebrates are at all conserved in ascidians. This will be greatly facilitated by the revised lineage tree presented in chapter 3 which allows for the precise identification of A-line cells at each time point between the initial tailbud and mid-tailbud stages. A careful look at the expression patterns of *FoxB, Otx, Pax6, and Engrailed* during this period will be a key first step assessing the relationship between the A9.14 lineage and vertebrate diencephalon.

While co-expression of *FoxB*, *Otx*, and *Pax6* is suggestive of diencephalon homology, it will also be critical to compare the sites of diencephalon embryonic origin for vertebrates and ascidians. In ascidians, *FoxB* is initially expressed in all A-line neural cells at the early gastrula stage, but quickly becomes restricted to A9.14 derivatives by the mid-gastrula stage (Imai et al., 2004; Yasuo and Hudson, 2007). Based on our revised lineages (chapter 3) and in-situ hybridizations, it seems that expression persists in A9.14 derivatives until the mid-tailbud stage and may also reactivate in derivatives of A10.64. During neurulation these same cells proliferate and move from the posterior neural plate to the middle of the sensory vesicle. In Xenopus embryos, *FoxB* expression follows a similar pattern (Gamse and Sive, 2001). During the middle of gastrulation it is expressed in the posterior most part of the neural plate adjacent to the blastopore. By the end of gastrulation its expression is present in regions fated to become diencephalon, midbrain, and hindbrain, and is more weakly expressed in regions fated to become spinal cord and tailbud. Eventually its expression is limited to two stripes in the CNS, including one in the territory fated to become the diencephalon and mesencephalon. What remains is to establish whether early vertebrate *FoxB* expressing cells are the same cells that express these genes during tailbud stages, and whether these cells eventually contribute to the diencephalon. If so, it would represent strong evidence that the A9.14 lineage in ascidians is evolutionarily linked to the vertebrate diencephalon.

Floor plate intercalation and lateral stacking

Although great progress has been made in our understanding of epithelial cell movements, there remains much that we don't know. The simplicity of ascidian neurulation may provide an opportunity in this area. Particularly intriguing is the differential expression of cadherins between the floor plate and lateral cells. Specifically, *Ci-d1-protocadherin-like* is expressed in floor plate cells during neurulation, while *Ci-Flamingo* is expressed in lateral cells (Noda and Satoh, 2008). Investigating how these

genes influence the stacking and intercalary behavior of these structures is sure to yield insight into the importance of differential cadherin expression on tissue architecture. As noted above, it is interesting that ci-*Flamingo* is not expressed in the floor-plate, as it is generally seen as a key component of the planar cell polarity pathway involved in intercalary behavior (Nishimura et al., 2012; Walck-Shannon and Hardin, 2013). Taken together with the use non-canonical FGF signaling during floor plate midline convergence, a deeper examination of this behavior might provide new insights into the diverse ways in which epithelial cell behaviors are coordinated.

A more comprehensive understanding of the links between signaling, cell specification, and morphogenesis will require looking at the full complement of genes expressed by the different A-line cell populations during neurulation. Luckily, single cell RNA-seq technology is becoming increasingly common and offers a promising solution to gather expression data from small cell populations such as those of the *Ciona* neural plate. The main difficulty at present is a lack of enhancers which drive expression exclusively in the different A-line neural populations. Possible solutions to this difficulty include selecting cells from embryos where all A-line cells have been transformed to adopt a particular behavior and/or the use of photoconvertible reporters to uniquely mark cells of the A-line neural plate, a technique which has been successfully applied to trace the A-line photoreceptor lineage (Oonuma et al., 2016). Uncovering the genes downstream of the FGF and Nodal signals which coordinate neural tube morphogenesis is the first step in opening the “black box” linking specification and cell movement. Completing this connection will require significant work and experimental ingenuity, but it seems possible that we may one day have a comprehensive understanding of how cells self-organize into the neural tube during ascidian neurulation.

Figure 19

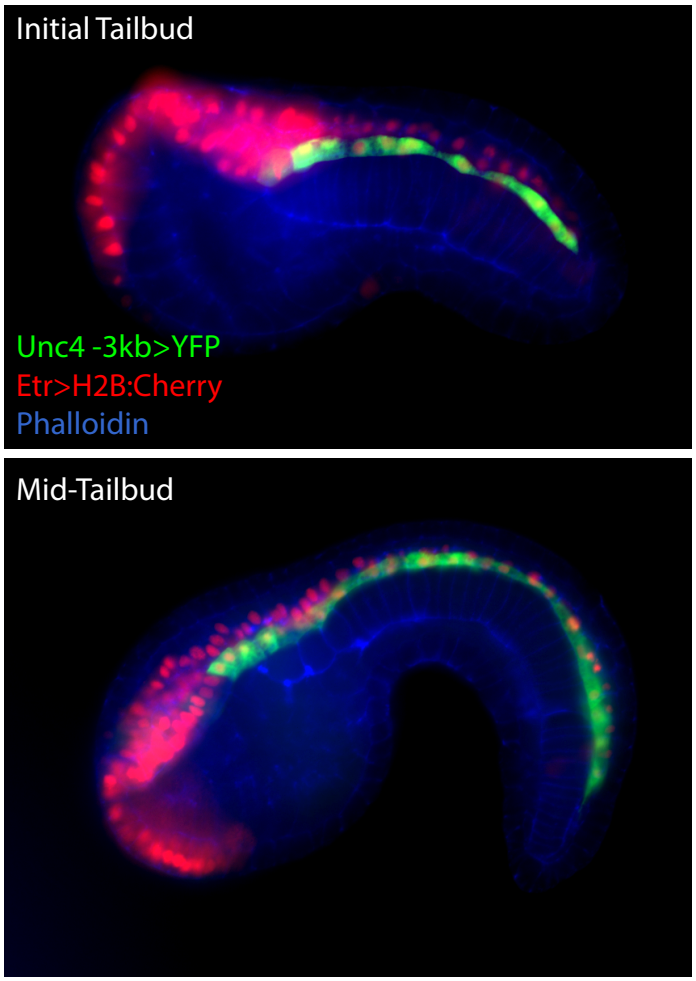

Unc4 enhancer. Fluorescent image of initial and mid-tailbud stage embryos electroporated with the Unc4 -3kb enhancer driving expression of YFP in the floor plate, together with Etr>H2B:Cherry.

REFERENCES

Bertrand, V., Hudson, C., Caillol, D., Popovici, C. and Lemaire, P. (2003). Neural Tissue in Ascidian Embryos Is Induced by FGF9/16/20, Acting via a Combination of Maternal GATA and Ets Transcription Factors. *Cell* **115**, 615–627.

Böttcher, R. T. and Niehrs, C. (2005). Fibroblast growth factor signaling during early vertebrate development. *Endocr. Rev.* **26**, 63–77.

Chabry, L. (1887). Embryologie normale et teratologique des Ascidies simples. *J. Anat. Physiol.* **23**, 167–319.

Christiaen, L., Davidson, B., Kawashima, T., Powell, W., Nolla, H., Vranizan, K. and Levine, M. (2008). The transcription/migration interface in heart precursors of Ciona intestinalis. *Science* **320**, 1349–1352.

Christiaen, L., Stolfi, A., Davidson, B. and Levine, M. (2009a). Spatio-temporal intersection of Lhx3 and Tbx6 defines the cardiac field through synergistic activation of Mesp. *Dev. Biol.* **328**, 552–560.

Christiaen, L., Wagner, E., Shi, W. and Levine, M. (2009b). Isolation of sea squirt (Ciona) gametes, fertilization, dechorionation, and development. *Cold Spring Harb. Protoc.*

Christiaen, L., Wagner, E., Shi, W. and Levine, M. (2009c). Electroporation of Transgenic DNAs in the Sea Squirt Ciona. *Cold Spring Harb. Protoc.* **2009**, pdb.prot5345-prot5345.

Cole, A. G. and Meinertzhagen, I. A. (2004). The central nervous system of the ascidian larva: Mitotic history of cells forming the neural tube in late embryonic Ciona intestinalis. *Dev. Biol.* **271**, 239–262.

Conklin, E. G. (1905). The Organization and Cell-Lineage of the Ascidian Egg. *Proc. Acad. Nat. Sci. Philadelphia* **13**, 1–119.

Corbo, J. C., Erives, a, Di Gregorio, a, Chang, a and Levine, M. (1997). Dorsoventral patterning of the vertebrate neural tube is conserved in a protochordate. *Development* **124**, 2335–2344.

Dal-Pra, S., Thisse, C. and Thisse, B. (2011). FoxA transcription factors are essential for the development of dorsal axial structures. *Dev. Biol.* **350**, 484–495.

Davidson, B., Shi, W., Beh, J., Christiaen, L. and Levine, M. (2006). FGF signaling delineates the cardiac progenitor field in the simple chordate , Ciona intestinalis. **4**, 2728–2738.

Delsuc, F., Brinkmann, H., Chourrout, D. and Philippe, H. (2006). Tunicates and not cephalochordates are the closest living relatives of vertebrates. *Nature* **439**, 965–968.

Denker, E., Sehring, I. M., Dong, B., Audisso, J., Mathiesen, B. and Jiang, D. (2015). Regulation by a TGFβ-ROCK-actomyosin axis secures a non-linear lumen expansion that is essential for tubulogenesis. *Development* **142**, 1639–50.

Di Gregorio, A., Harland, R. M., Levine, M. and Casey, E. S. (2002). Tail morphogenesis in the ascidian, Ciona intestinalis, requires cooperation between notochord and muscle. *Dev. Biol.* **244**, 385–395.

Dufour, H. D., Chettouh, Z., Deyts, C., de Rosa, R., Goridis, C., Joly, J.-S. and Brunet, J.-F. (2006). Precraniate origin of cranial motoneurons. *Proc. Natl. Acad. Sci. U. S. A.* **103**, 8727–8732.

Ettensohn, C. a. (2013). Encoding anatomy: Developmental gene regulatory networks and morphogenesis. *Genesis* **51**, 383–409.

Gainous, T. B., Wagner, E. and Levine, M. (2014). Diverse ETS transcription factors mediate FGF signaling in the Ciona anterior neural plate. *Dev. Biol.* **399**, 218–225.

Gamse, J. T. and Sive, H. (2001). Early anteroposterior division of the presumptive neurectoderm in Xenopus. *Mech. Dev.* **104**, 21–36.

Hashimoto, H., Enomoto, T., Kumano, G. and Nishida, H. (2011). The transcription factor FoxB mediates temporal loss of cellular competence for notochord induction in ascidian embryos. *Development* **138**, 2591–2600.

Hashimoto, H., Robin, F. B., Sherrard, K. M. and Munro, E. M. (2015). Sequential contraction and exchange of apical junctions drives zippering and neural tube closure in a simple chordate. *Dev Cell* **32**, 241–255.

Haupaix, N., Stolfi, A., Sirour, C., Picco, V., Levine, M., Christiaen, L. and Yasuo, H. (2013). p120RasGAP mediates ephrin/Eph-dependent attenuation of FGF/ERK signals during cell fate specification in ascidian embryos. *Development* **140**, 4347–52.

Hudson, C. and Lemaire, P. (2001). Induction of anterior neural fates in the ascidian Ciona intestinalis. *Mech. Dev.* **100**, 189–203.

Hudson, C. and Yasuo, H. (2005). Patterning across the ascidian neural plate by lateral Nodal signalling sources. *Development* **132**, 1199–210.

Hudson, C., Darras, S., Caillol, D., Yasuo, H. and Lemaire, P. (2003). A conserved role for the MEK signalling pathway in neural tissue specification and posteriorisation in the invertebrate chordate, the ascidian Ciona intestinalis. *Development* **130**, 147–159.

Hudson, C., Lotito, S. and Yasuo, H. (2007). Sequential and combinatorial inputs from Nodal, Delta2/Notch and FGF/MEK/ERK signalling pathways establish a grid-like organisation of distinct cell identities in the ascidian neural plate. *Development* **134**, 3527–3537.

Hudson, C., Kawai, N. and Negishi, T. (2013). b -Catenin-Driven Binary Fate Specification Segregates Germ Layers in Ascidian Embryos. *Curr. Biol.* **23**, 491–495.

Hudson, C., Sirour, C. and Yasuo, H. (2015). Snail mediates medial–lateral patterning of the ascidian neural plate. *Dev. Biol.* **403**, 1–8.

Hudson, C., Sirour, C. and Yasuo, H. (2016). Co-expression of Foxa . a , Foxd and Fgf9 / 16 / 20 defines a transient mesendoderm regulatory state in ascidian embryos. 1–17.

Ikuta, T. and Saiga, H. (2007). Dynamic change in the expression of developmental genes in the ascidian central nervous system: Revisit to the tripartite model and the origin of the midbrain-hindbrain boundary region. *Dev. Biol.* **312**, 631–643.

Imai, K. S., Hino, K., Yagi, K., Satoh, N. and Satou, Y. (2004). Gene expression profiles of transcription factors and signaling molecules in the ascidian embryo: towards a comprehensive understanding of gene networks. *Development* **131**, 4047–4058.

Imai, K. S., Levine, M., Satoh, N. and Satou, Y. (2006). Regulatory Blueprint for a Chordate Embryo. *Science.* **312**, 1183–1187.

Imai, K. S., Stolfi, A., Levine, M. and Satou, Y. (2009). Gene regulatory networks underlying the compartmentalization of the Ciona central nervous system. *Development* **136**, 285–293.

Inazawa, T., Okamura, Y. and Takahashi, K. (1998). Basic fibroblast growth factor induction of neuronal ion channel expression in ascidian ectodermal blastomeres.

Kengaku, M. and Okamoto, H. (1993). Basic fibroblast growth factor induces differentiation of neural tube and neural crest lineages of cultured ectoderm cells from Xenopus gastrula. *Development* **119**, 1067–78.

Kengaku, M. and Okamoto, H. (1995). bFGF as a possible morphogen for the anteroposterior axis of the central nervous system in Xenopus. *Development* **121**, 3121–30.

Kim, G. J. and Nishida, H. (2001). Role of the FGF and MEK signaling pathway in the ascidian embryo. 521–533.

Kodama, H., Miyata, Y., Kuwajima, M., Izuchi, R., Kobayashi, A., Gyoja, F., Onuma, T. A., Kumano, G. and Nishida, H. (2016). Redundant mechanisms are involved in suppression of default cell fates during embryonic mesenchyme and notochord induction in ascidians. *Dev. Biol.* **416**, 162–172.

Kourakis, M. J., Reeves, W., Newman-Smith, E., Maury, B., Abdul-Wajid, S. and Smith, W. C. (2014). A one-dimensional model of PCP signaling: polarized cell behavior in the notochord of the ascidian Ciona. *Dev. Biol.* **395**, 120–30.

Kowalevsky, A. (1866). Entwickelungsgeschichte der einfachen Ascidien. *Mem. L'acad. Imp. Sci. St. Petersbg.* **10**, 1–19.

Kusakabe, T. G. and Tsuda, M. (2007). Photoreceptive systems in ascidians. *Photochem. Photobiol.* **83**, 248–252.

Lemaire, P., Bertrand, V. and Hudson, C. (2002). Early steps in the formation of neural tissue in ascidian embryos. *Dev. Biol.* **252**, 151–169.

Lumsden, a and Krumlauf, R. (1996). Patterning the vertebrate neuraxis. *Science* **274**, 1109–1115.

Matsumoto, J., Kumano, G. and Nishida, H. (2007). Direct activation by Ets and Zic is required for initial expression of the Brachyury gene in the ascidian notochord. *Dev. Biol.* **306**, 870–882.

Miroux, B. and Walker, J. E. (1996). Over-production of proteins in Escherichia coli: mutant hosts that allow synthesis of some membrane proteins and globular proteins at high levels. *J. Mol. Biol.* **260**, 289–98.

Mita, K. and Fujiwara, S. (2007). Nodal regulates neural tube formation in the Ciona intestinalis embryo. *Dev. Genes Evol.* **217**, 593–601.

Mita, K., Koyanagi, R., Azumi, K., Sabau, S. V, Fujiwara, S., Mita, K., Koyanagi, R., Azumi, K., Sabau, S. V and Fujiwara, S. (2010). Identification of Genes Downstream of Nodal in the Ciona intestinalis Embryo Identification of Genes Downstream of Nodal in the Ciona intestinalis Embryo. **27**, 69–75.

Miyamoto, D. M. and Crowther, R. J. (1985). Formation of the notochord in living ascidian embryos. *J. Embryol. Exp. Morphol.* **86**, 1–17.

Moret, F., Christiaen, L., Deyts, C., Blin, M., Vernier, P. and Joly, J.-S. (2005). Regulatory gene expressions in the ascidian ventral sensory vesicle: evolutionary relationships with the vertebrate hypothalamus. *Dev. Biol.* **277**, 567–79.

Nakamura, M. J., Terai, J., Okubo, R., Hotta, K. and Oka, K. (2012). Three-dimensional anatomy of the Ciona intestinalis tailbud embryo at single-cell resolution. *Dev Biol* **372**, 274–84.
Nakatani, Y. and Nishida, H. (1994). Induction of notochord during ascidian embryogenesis. *Dev. Biol.* **166**, 289–99.
Nakatani, Y. and Nishida, H. (1997). Ras is an essential component for notochord formation during ascidian embryogenesis. **68**, 81–89.
Nicol, D. and Meinertzhagen, I. A. (1988a). Development of the Central Nervous System of the Larva of the Ascidian, Ciona intestinalis L. II. Neural Plate Morphogenesis and cell lineages during neurulation. *Dev. Biol.* **130**, 737–766.
Nicol, D. and Meinertzhagen, I. A. (1988b). Development of the central nervous system of the larva of the ascidian, Ciona intestinalis L. I. The early lineages of the neural plate. *Dev. Biol.* **130**, 721–36.
Nicol, D. and Meinertzhagen, I. a (1991). Cell counts and maps in the larval central nervous system of the ascidian Ciona intestinalis (L.). *J. Comp. Neurol.* **309**, 415–29.
Nishida, H. (1986). Cell Division Pattern during Gastrulation of the Ascidian,. *Dev. Growth Differ.* **28**, 191–201.
Nishida, H. (1987). Cell lineage analysis in ascidian embryos by intracellular injection of a tracer enzyme. III. Up to the tissue restricted stage. *Dev. Biol.* **121**, 526–41.
Nishida, H. (1992). D elopmental Biology of fully dissociated cells of the ascidian embryo. 81–87.
Nishida, H. and Sawada, K. (2001). macho-1 encodes a localized mRNA in ascidian eggs that specifies muscle fate during embryogenesis. *Nature* **409**, 724-9.
Nishimura, T., Honda, H. and Takeichi, M. (2012). Planar Cell Polarity Links Axes of Spatial Dynamics in Neural-Tube Closure. *Cell* **149**, 1084–1097.
Noda, T. and Satoh, N. (2008). A comprehensive survey of cadherin superfamily gene expression patterns in Ciona intestinalis. *Gene Expr. Patterns* **8**, 349–56.
Oda, I. and Saiga, H. (2001). Hremx, the ascidian homologue of ems/emx, is expressed in the anterior and posterior-lateral epidermis but not in the central nervous system during embryogenesis. *Dev. Genes Evol.* **211**, 291–8.
Oda-Ishii, I., Kubo, A., Kari, W., Suzuki, N., Rothbächer, U. and Satou, Y. (2016). A Maternal System Initiating the Zygotic Developmental Program through Combinatorial Repression in the Ascidian Embryo. *PLoS Genet.* **12**, 1–24.
Ogura, Y., Sakaue-Sawano, A., Nakagawa, M., Satoh, N., Miyawaki, A. and Sasakura, Y. (2011). Coordination of mitosis and morphogenesis: role of a prolonged G2 phase during chordate neurulation. *Development* **138**, 577–587.
Okado, H. and Takahashi, K. (1988). A simple “neural induction” model with two interacting cleavage-arrested. **85**, 6197–6201.
Oonuma, K., Tanaka, M., Nishitsuji, K., Kato, Y., Shimai, K. and Kusakabe, T. G. (2016). Revised lineage of larval photoreceptor cells in Ciona reveals archetypal collaboration between neural tube and neural crest in sensory organ formation. *Dev. Biol.* 1–8.
Ortolani, G., Patricolo, E. and Mansueto, C. (1979). Trypsin-induced cell surface changes in ascidian embryonic cells: regulation of differentiation of a tissue-specific protein. *Exp. Cell Res.* **122**, 137–47.

Peyrot, S. M., Wallingford, J. B. and Harland, R. M. (2011). A revised model of Xenopus dorsal midline development: Differential and separable requirements for Notch and Shh signaling. *Dev. Biol.* **352**, 254–266.

Picco, V., Hudson, C. and Yasuo, H. (2007). Ephrin-Eph signalling drives the asymmetric division of notochord/neural precursors in Ciona embryos. *Development* **134**, 1491–7.

Razy-Krajka, F., Brown, E. R., Horie, T., Callebert, J., Sasakura, Y., Joly, J. S., Kusakabe, T. G. and Vernier, P. (2012). Monoaminergic modulation of photoreception in ascidian: evidence for a proto-hypothalamo-retinal territory. *BMC Biol* **10**, 45.

Rose, S. M. (1939). Embryonic Induction in the Ascidia. *Biol. Bull.* **77**, 216–232.

Sasakura, Y., Shoguchi, E., Takatori, N., Wada, S., Meinertzhagen, I. a., Satou, Y. and Satoh, N. (2003). A genomewide survey of developmentally relevant genes in Ciona intestinalis. X. Genes for cell junctions and extracellular matrix. *Dev. Genes Evol.* **213**, 303–313.

Satoh, N. (1984). Studies on the Cytoplasmic Determinant for Muscle Cell Differentiation in Ascidian Embryos : An Attempt at Transplantation of the Myoplasm. **26**, 43–48.

Satou, Y., Sasakura, Y., Yamada, L., Imai, K. S., Satoh, N. and Degnan, B. (2003). A genomewide survey of developmentally relevant genes in Ciona intestinalis. V. Genes for receptor tyrosine kinase pathway and Notch signalling pathway. *Dev. Genes Evol.* **213**, 254–263.

Schindelin, J., Arganda-Carreras, I., Frise, E., Kaynig, V., Longair, M., Pietzsch, T., Preibisch, S., Rueden, C., Saalfeld, S., Schmid, B., et al. (2012). Fiji: an open-source platform for biological-image analysis. *Nat. Methods* **9**, 676–82.

Scholpp, S., Lohs, C. and Brand, M. (2003). Engrailed and Fgf8 act synergistically to maintain the boundary between diencephalon and mesencephalon. *Development* **130**, 4881–4893.

Sherrard, K., Robin, F., Lemaire, P. and Munro, E. (2010). Sequential activation of apical and basolateral contractility drives ascidian endoderm invagination. *Curr. Biol.* **20**, 1499–510.

Shi, W., Peyrot, S. M., Munro, E. and Levine, M. (2009). FGF3 in the floor plate directs notochord convergent extension in the Ciona tadpole. *Development* **136**, 23–8.

Shindo, A. and Wallingford, J. B. (2014). PCP and septins compartmentalize collective cell movement. *Science (80-.).* **343**, 649–652.

Stolfi, A. and Levine, M. (2011). Neuronal subtype specification in the spinal cord of a protovertebrate. *Development* **138**, 995–1004.

Stolfi, a., Wagner, E., Taliaferro, J. M., Chou, S. and Levine, M. (2011). Neural tube patterning by Ephrin, FGF and Notch signaling relays. *Development* **138**, 5429–5439.

Stolfi, A., Ryan, K., Meinertzhagen, I. A. and Christiaen, L. (2015). Migratory neuronal progenitors arise from the neural plate borders in tunicates. *Nature* **527**, 371–374.

Swalla, B. J. and Smith, A. B. (2008). Deciphering deuterostome phylogeny: molecular, morphological and palaeontological perspectives. *Philos. Trans. R. Soc. Lond. B. Biol. Sci.* **363**, 1557–68.

Taniguchi, K. and Nishida, H. (2004). Tracing cell fate in brain formation during embryogenesis of the ascidian Halocynthia roretzi. *Dev. Growth Differ.* **46**, 163–80.

Veeman, M. T., Nakatani, Y., Hendrickson, C., Ericson, V., Lin, C. and Smith, W. C. (2008). Chongmague reveals an essential role for laminin-mediated boundary formation in chordate convergence and extension movements. *Development* **135**, 33–41.

Veeman, M. T., Newman-Smith, E., El-Nachef, D. and Smith, W. C. (2010). The ascidian mouth opening is derived from the anterior neuropore: Reassessing the mouth/neural tube relationship in chordate evolution. *Dev. Biol.* **344**, 138–149.

Wada, H., Saiga, H., Satoh, N. and Holland, P. W. (1998). Tripartite organization of the ancestral chordate brain and the antiquity of placodes: insights from ascidian Pax-2/5/8, Hox and Otx genes. *Development* **125**, 1113–1122.

Wagner, E. and Levine, M. (2012). FGF signaling establishes the anterior border of the Ciona neural tube. *Development* **139**, 2351–9.

Wagner, E., Stolfi, A., Gi Choi, Y. and Levine, M. (2014). Islet is a key determinant of ascidian palp morphogenesis. *Development* **141**, 3084–92.

Walck-Shannon, E. and Hardin, J. (2013). Cell intercalation from top to bottom. *Nat. Rev. Mol. Cell Biol.* **15**, 34–48.

Whittaker, J. R. (1982). Muscle lineage cytoplasm can change the developmental expression in epidermal lineage cells of ascidian embryos. *Dev. Biol.* **93**, 463–470.

Yasuo, H. and Hudson, C. (2007). FGF8/17/18 functions together with FGF9/16/20 during formation of the notochord in Ciona embryos. *Dev. Biol.* **302**, 92–103.

Material from the article:

Navarrete I.A., Levine M. (2016). Nodal and FGF coordinate ascidian neural tube morphogenesis. *Development* **143**, 4665-4675.

has been reproduced or adapted with permission.